

International Spring School on Forefront Alloys and Advanced Materials for Extreme Conditions

15 – 17 May 2017

Sardinia, Italy

Materials consolidation by high pressure in solid and liquid medium for extreme conditions

Dr. Mythili PRAKASAM

Engineer- CNRS

« Crystal Growth, High pressure, Sintering, Thin Films »

+

« Metallurgy and functional materials »

ICMCB-CNRS (UPR9048), France

National Center for Scientific Research (CNRS)

Mythili.prakasam@icmcb.cnrs.fr



Solid **Energy** **Exploratory** **Environment** **Modeling** **Optics** **Chemistry** **Matter** **Materials** **Condensed** **Nanomaterials** **Oxides** **Electronic** **Battery** **Supercritical** **Molecules** **Nanoparticles** **Functional** **Switchable** **Characterisation** **Métallurgy** **Fluoride** **Sintering** **Thin layers** **Formatting** **Multi-scale imaging** **Cristallogenesis** **High Pressure**

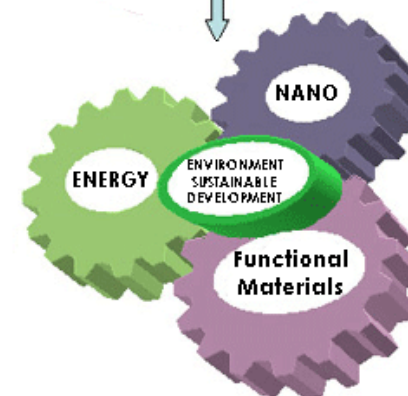
Competences

Solid State Chemistry
Materials Science
Molecular Science

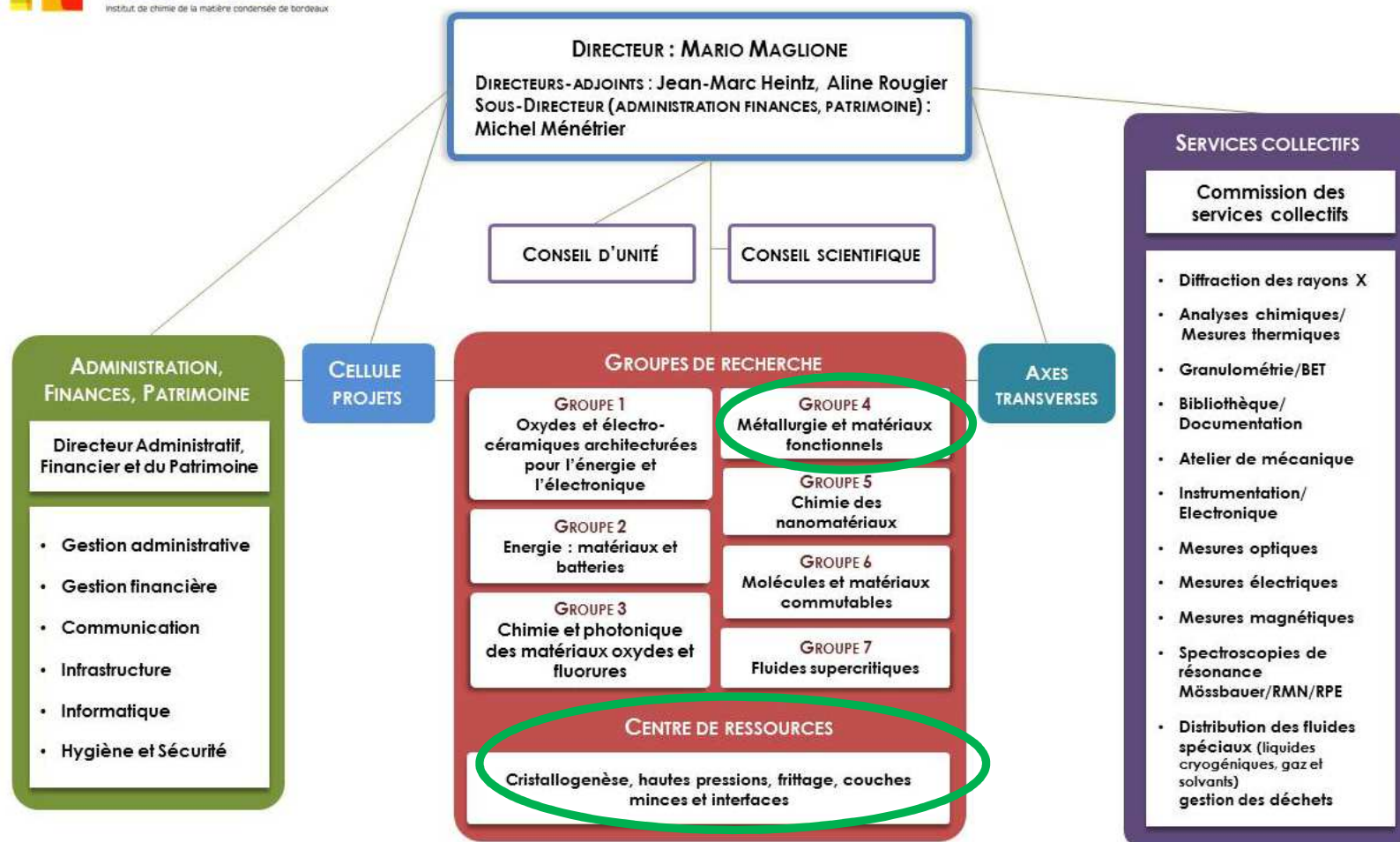
Facilities

synthesis
shaping
characterization

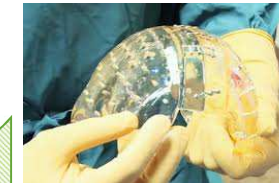
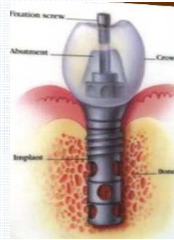
SPECIFIC TOPICS



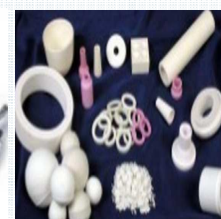
ORGANIGRAMME DE L'ICMCB



**B
i
o
c
e
r
a
m
i
c
s**



**Materials and
devices for
various medical
applications**





Laser cutting tools



Nose cone- heat seeking missiles



Night vision devices

Transparent ceramics applications

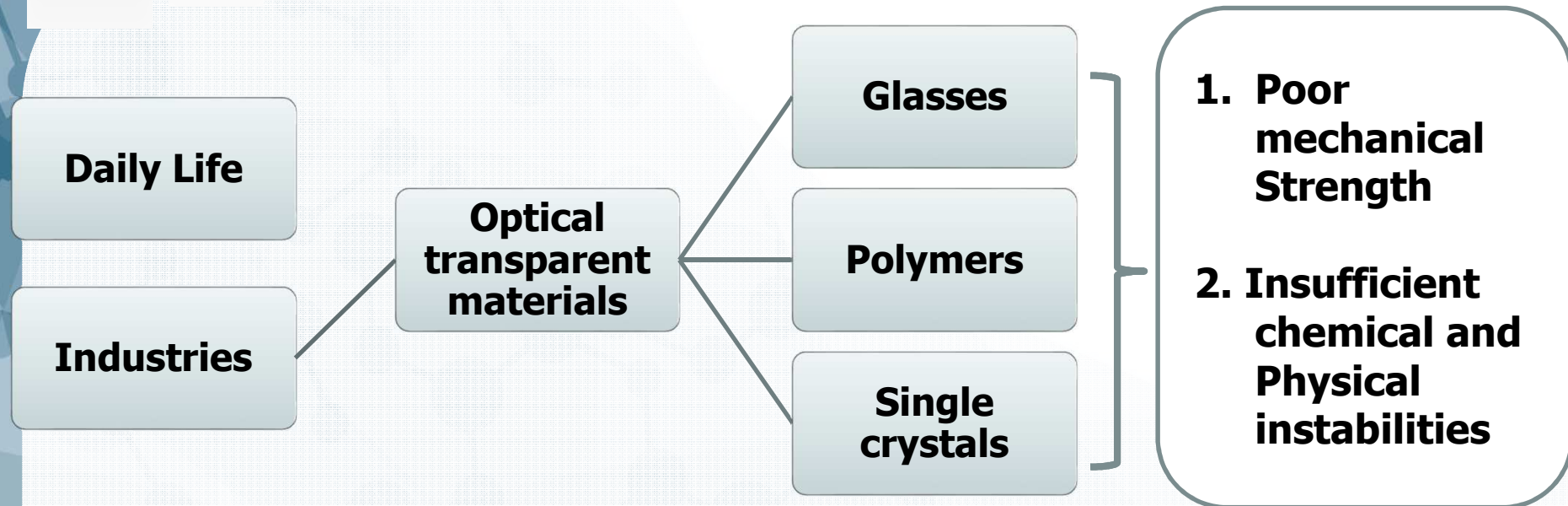


Armor/ window



Bullet shields

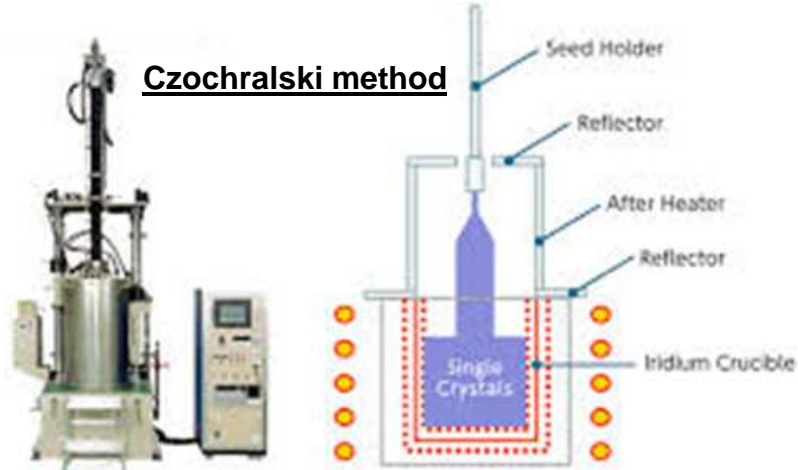
1. Introduction on optical transparent materials



- **Conventional transparent materials have a strong absorption in the IR range and usually possess melting points $< 600^{\circ}\text{C}$ - inhibits usage at higher temperatures**
- **Hence it was essential to develop new transparent materials that can be used for applications operating in harsh and extreme conditions**

Conventional crystal growth techniques

Czochralski method



Expensive components



Iridium and Platinum crucibles



→ Grown crystals are restricted by crucibles

1. Grown crystals are prone to defects and thermal stresses
2. Inhomogeneous/ segregation of dopants
3. Grown crystal predetermined by its crystalline structure

Bridgman method



1. Requires melting
2. May induce decomposition/phase changes in some compositions
3. Lengthy experiments



1. Additional cutting and processing
Required for fabrication of devices in required shapes
2. Wastage of material during cutting and polishing

Introduction on optical transparent materials

Traditionally used single crystals

Sapphire (Al_2O_3)
IR Windows

YAG
($\text{Y}_3\text{Al}_5\text{O}_{12}$)
Lasers

PZN-PT
($\text{PbZn}_{1/3}\text{Nb}_{2/3}\text{O}_3$ - PbTiO_3)
Electro-optics

**Growth of
single
crystals**

**Sophisticated
facilities**

**Time
consuming**

Expensive

Additional drawbacks of single crystals:

1. Shapes determined by lattice structures
2. Has shape of processing container and processing conditions
3. Machining of single crystals to meet specific applications is a difficult task
4. Difficulty of large scale production
5. Mechanical brittleness of some materials

Could transparent ceramics be advantageous over single crystals?

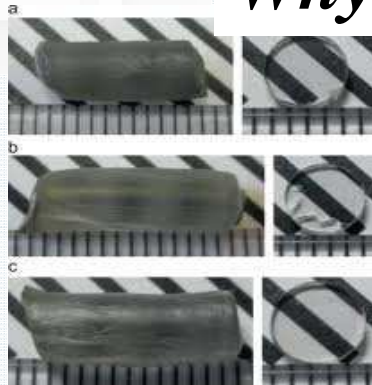
Advantages of transparent ceramics over single crystals

- ☐ Cost-effectiveness
- ☐ Large scale production
- ☐ Feasibility of shape controlling
- ☐ Better Mechanical properties

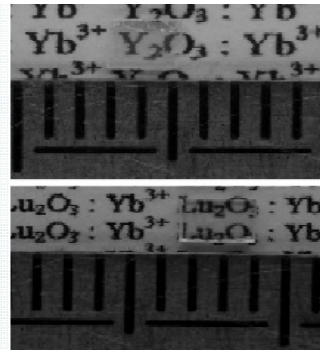
Ceramics: Densified polycrystalline grains with grain boundaries

Vital difference of single crystals and ceramics are various sites to scatter light

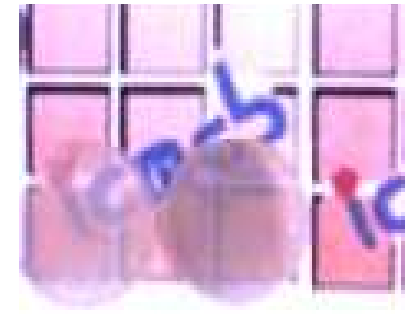
Why transparent ceramics over single crystals?



YAG crystal grown @ 1950°C

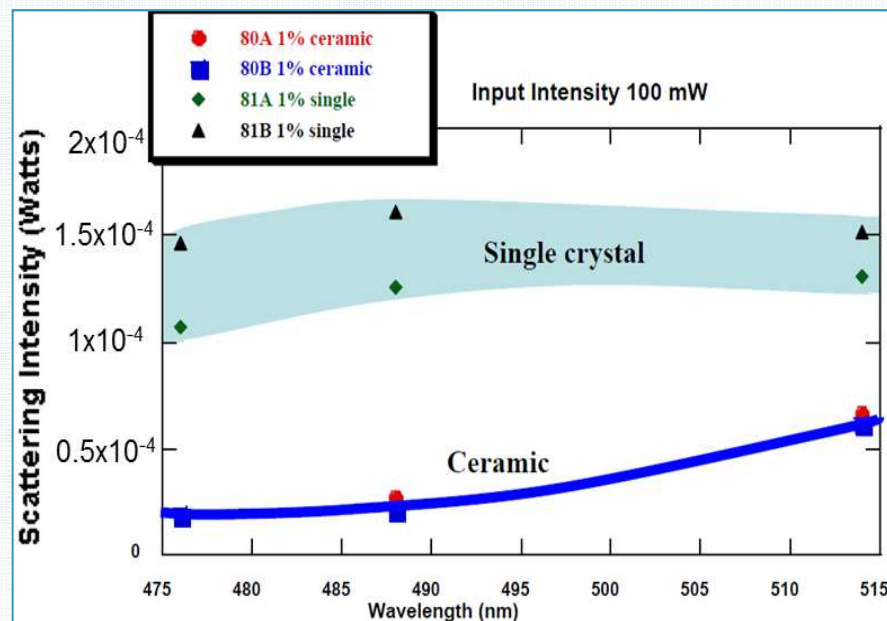


Sesquioxide crystal grown @ 1200°C by flux method

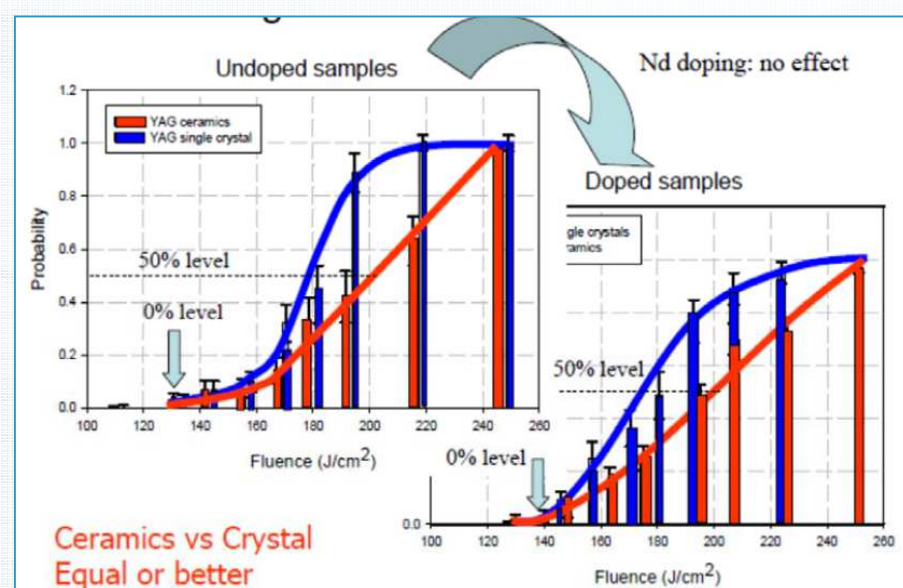


Yb:Lu₂O₃ ceramics -1400°C- 20 min

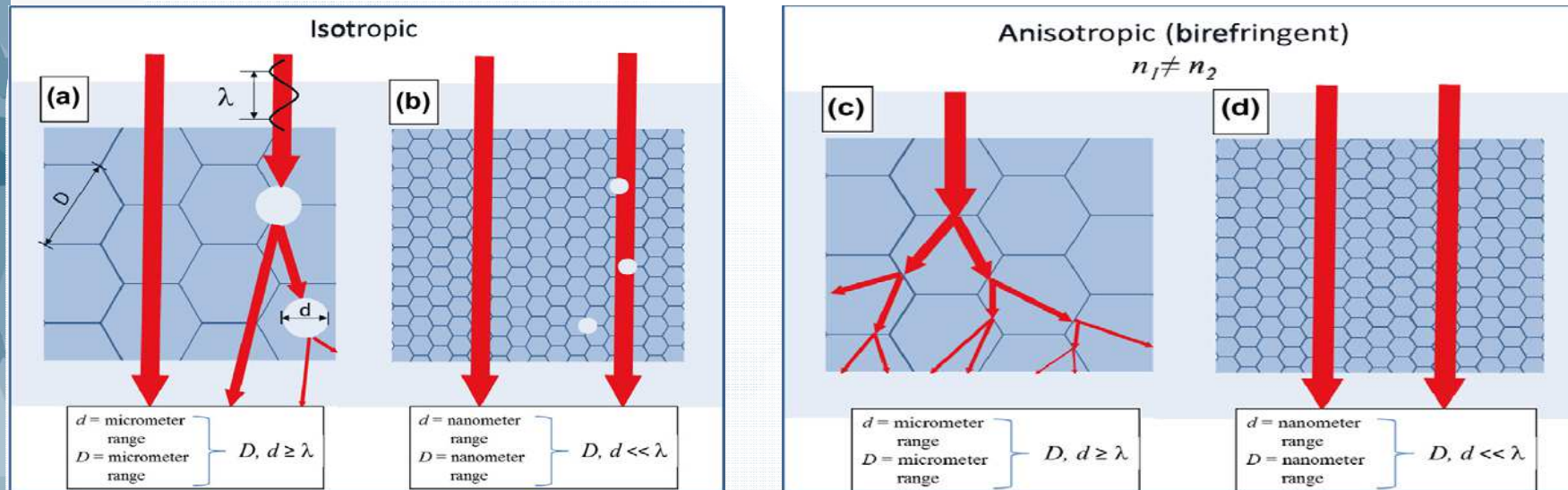
Demonstration of lower scattering loss in ceramic Nd:YAG



Laser damage threshold



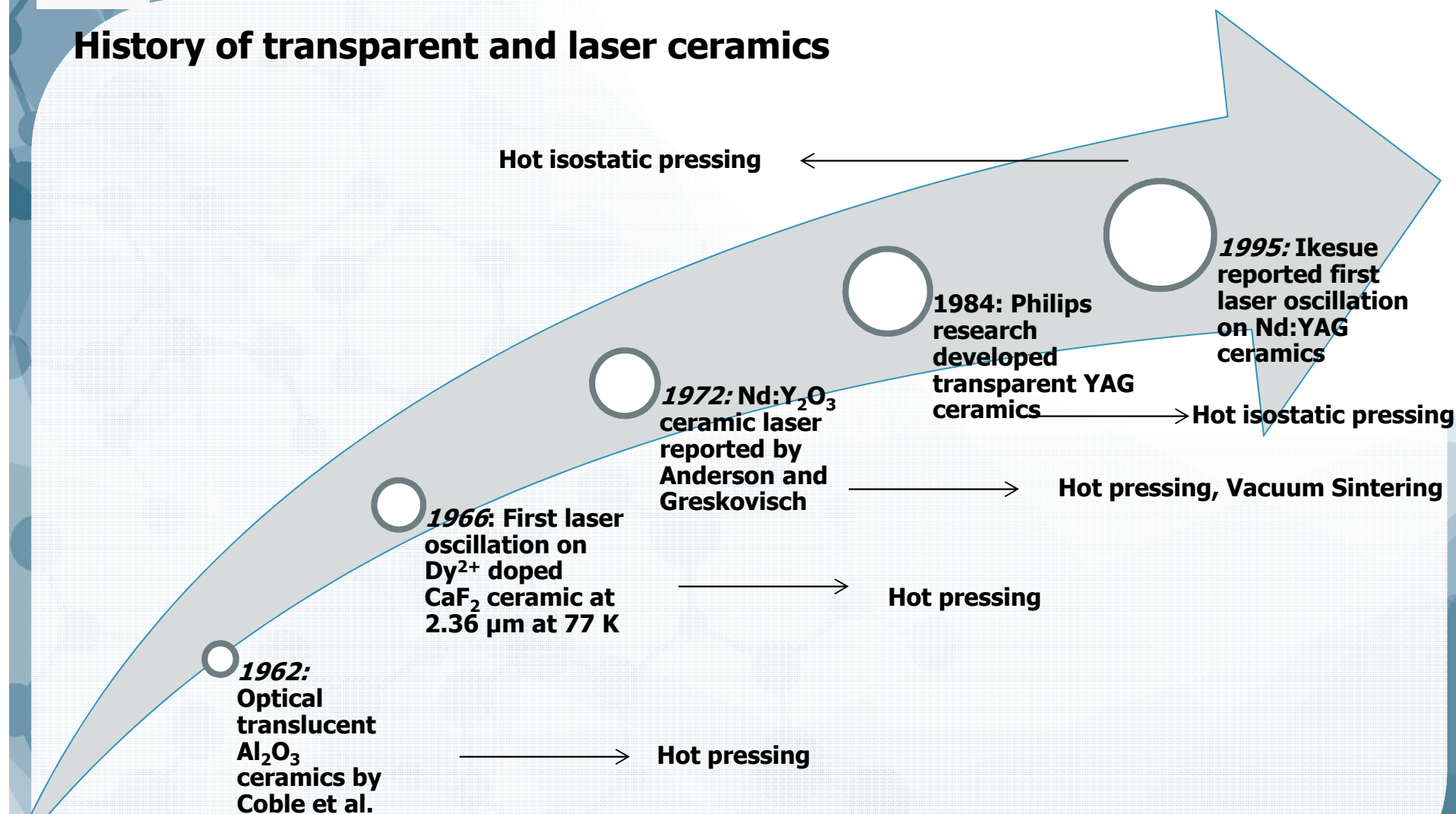
Role of microstructure on optical properties



Schematic representations of the interaction of light with polycrystalline ceramics.

- ❑ **Materials with cubic symmetry- refractive index 'n' similar in all directions- Isotropic**
 - **Isotropic material- Pore scattering efficiency depends on pore size**
 - ❖ pore size $\sim \mu\text{m}$ (i.e., Comparable to wavelength of light)- High scattering
 - ❖ pore size $< 100 \text{ nm}$, Interaction with visible light is minimal & optical transmittance increases
- ❑ **Materials with non-cubic symmetry- anisotropic/ birefringent**
 - **Grain size plays a more significant role**
 - ❖ **Light is scattered at each grain boundary**
 - ❖ **A strategy to improve transparency of an anisotropic material is to ensure nanometric grain sizes**

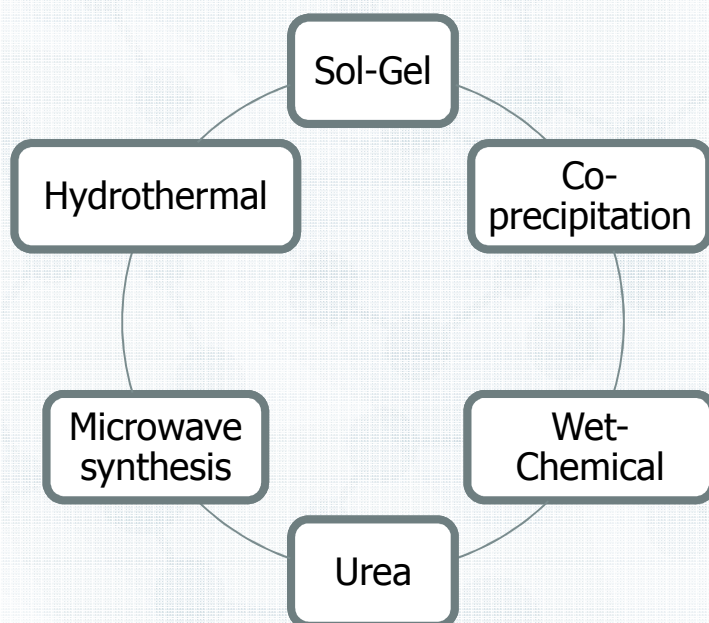
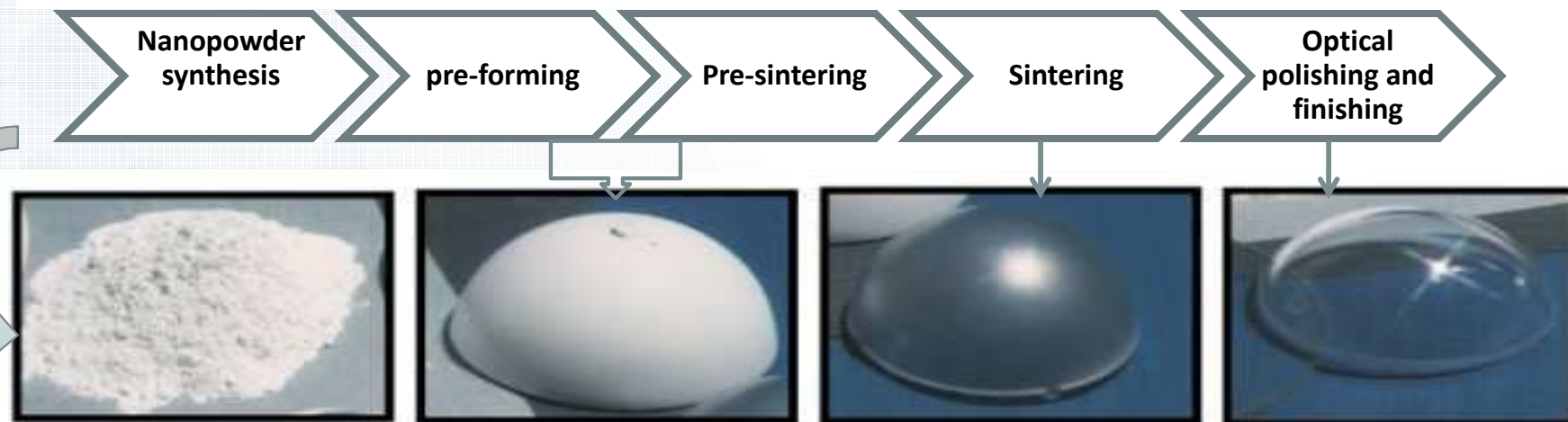
History of transparent and laser ceramics



References:

Carnall, E., et al Mater. Sci. Res., Vol. 3, pp. 165&173, 1966.
Coble, R.L., 1961, *J. Appl. Phys.*, vol. 32 (5), pp. 787-99.

Essential steps involved in fabrication of transparent ceramics



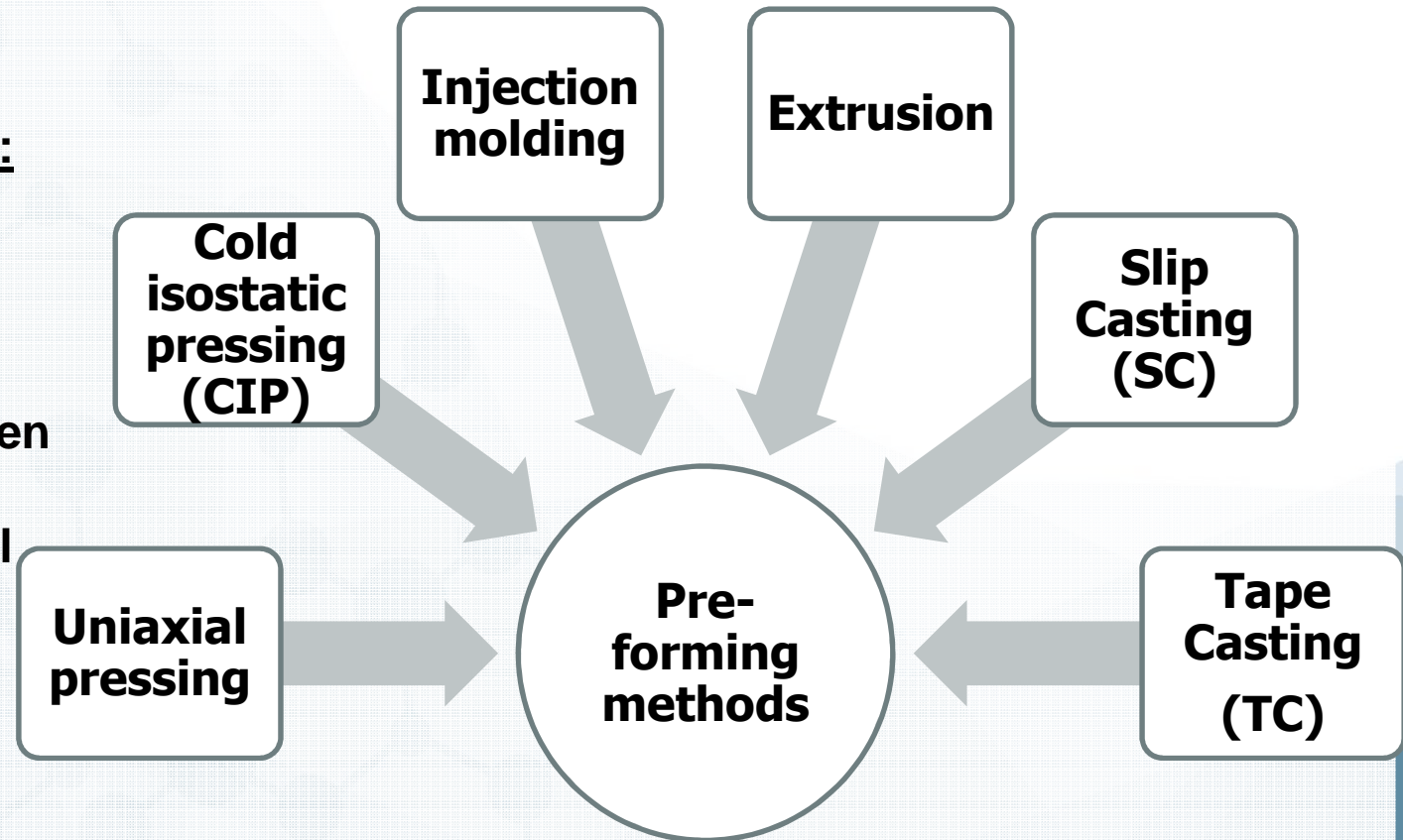
Various methods of nanopowder syntheses used for transparent ceramics

1. Nanopowders of the range 20 - 200 nm
2. Non-agglomeration of nanopowders
3. Free flowing powder
4. High purity

Pre-forming methods used for fabrication of transparent ceramics

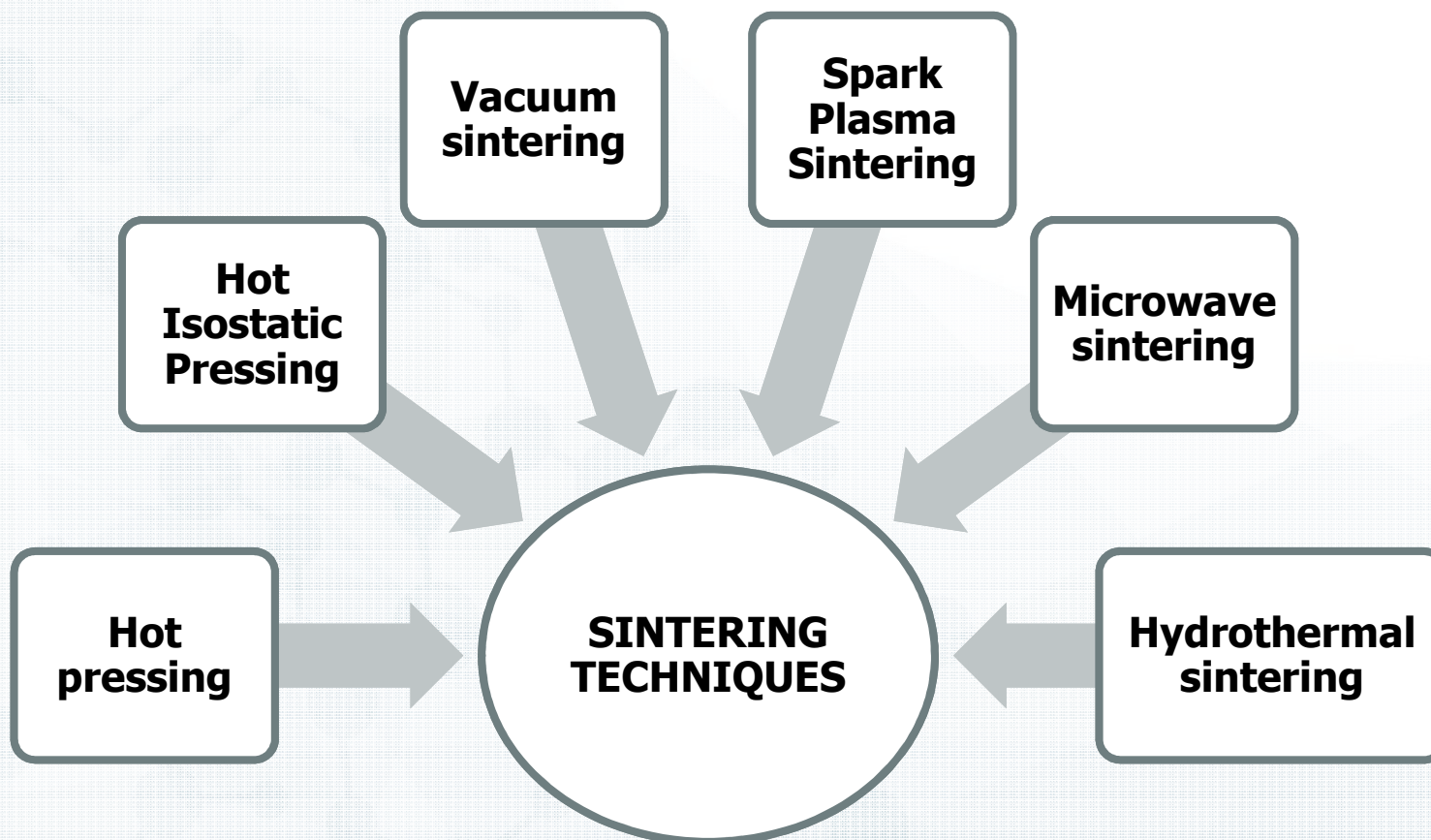
Advantages of pre-forming methods:

1. No pores formation,
2. Uniform/homogenous green body
3. Easy pore removal

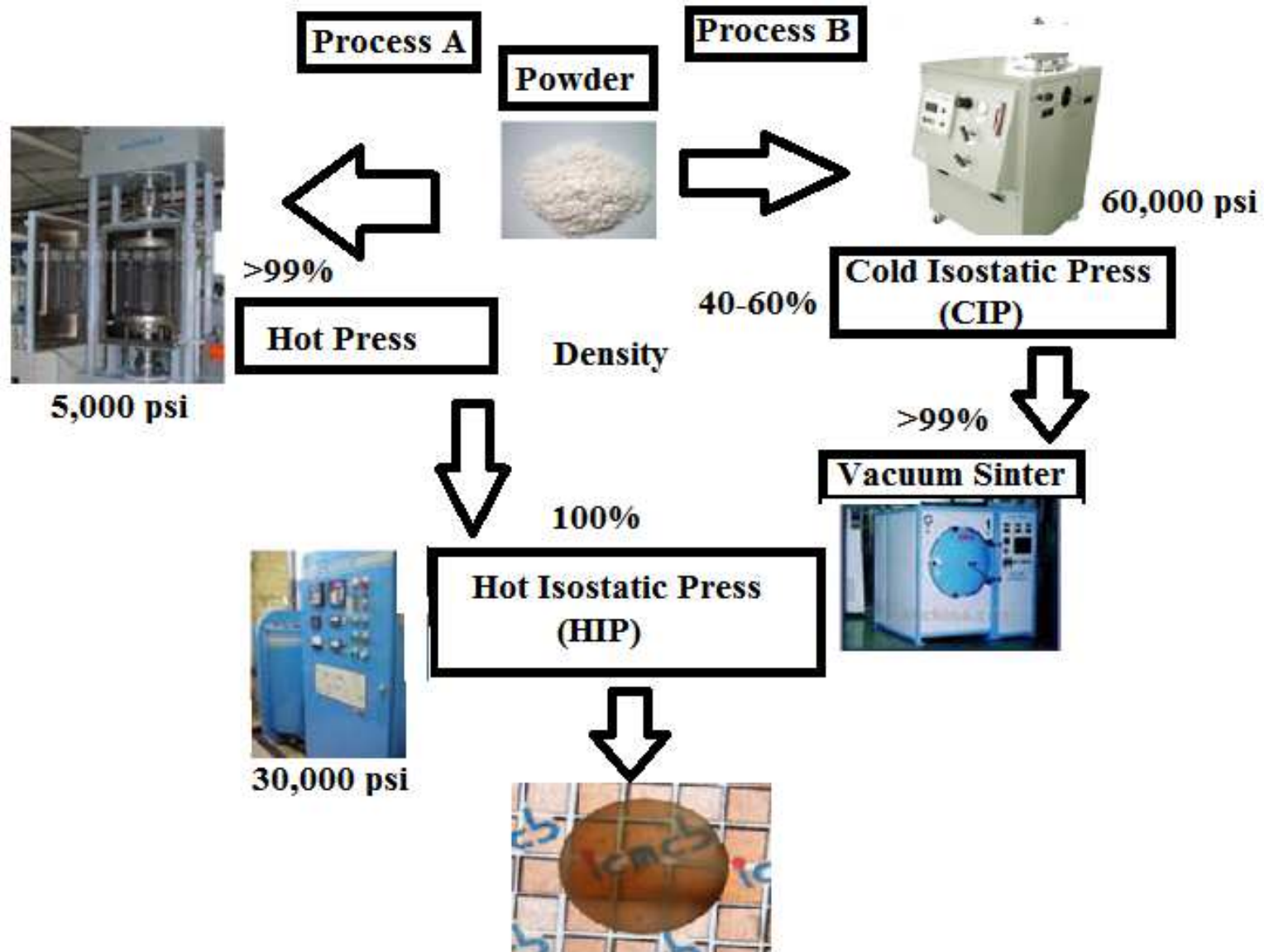


MOST FREQUENTLY USED PRE-FORMING METHODS : CIP, SC and TC.

Different sintering techniques employed to obtain transparent ceramics



General procedure for fabrication of transparent ceramics





Arc tube lamp



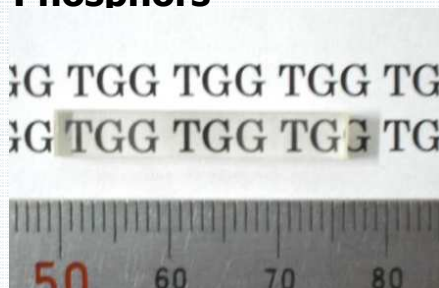
Electro-optics



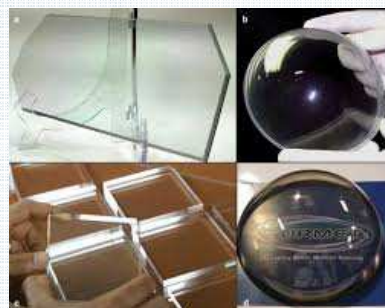
Laser ceramics



Scintillators and Phosphors



Faraday rotators



Domes and windows applications



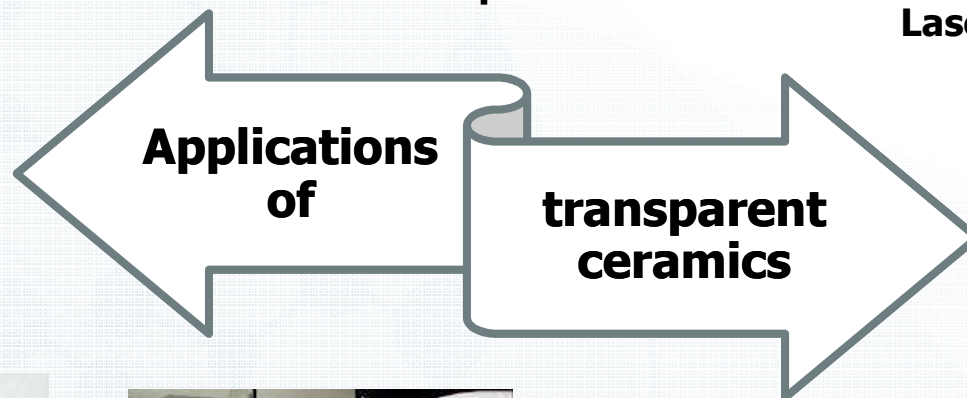
Infrared optic and lens



Armor applications

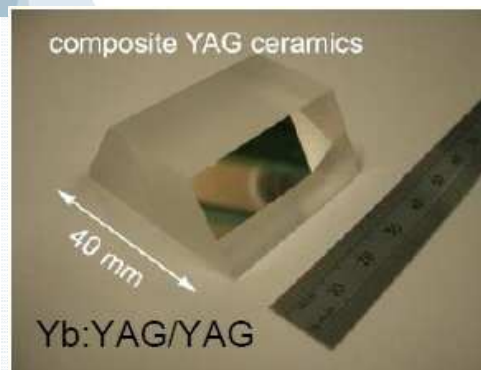


Small optical parts with complex structure





Composite material with different gradients of doping in Nd:Yb:YAG



Yb:YAG composite ceramic laser with a total reflection active mirror

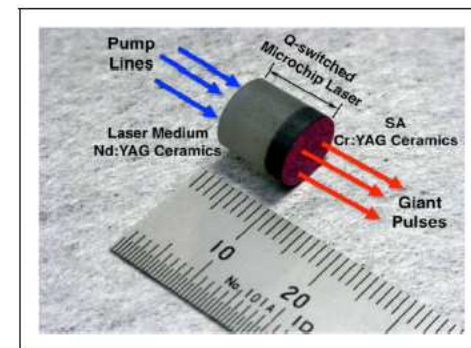
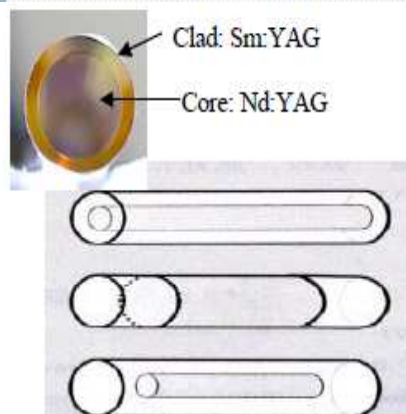


Photo of monolithic Nd:YAG/ Cr: YAG Composite ceramic chip



Composite Ceramic laser

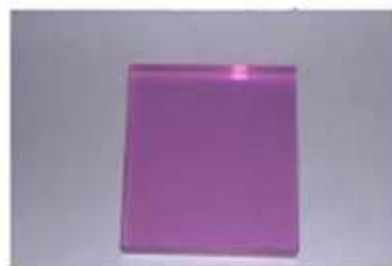
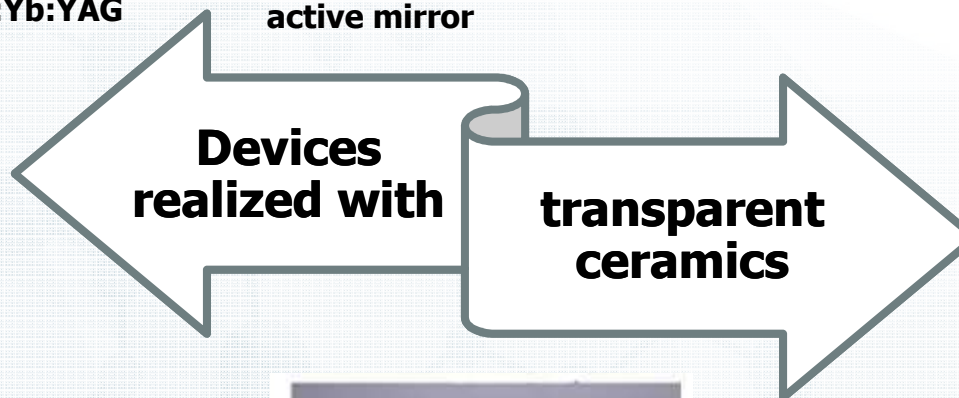
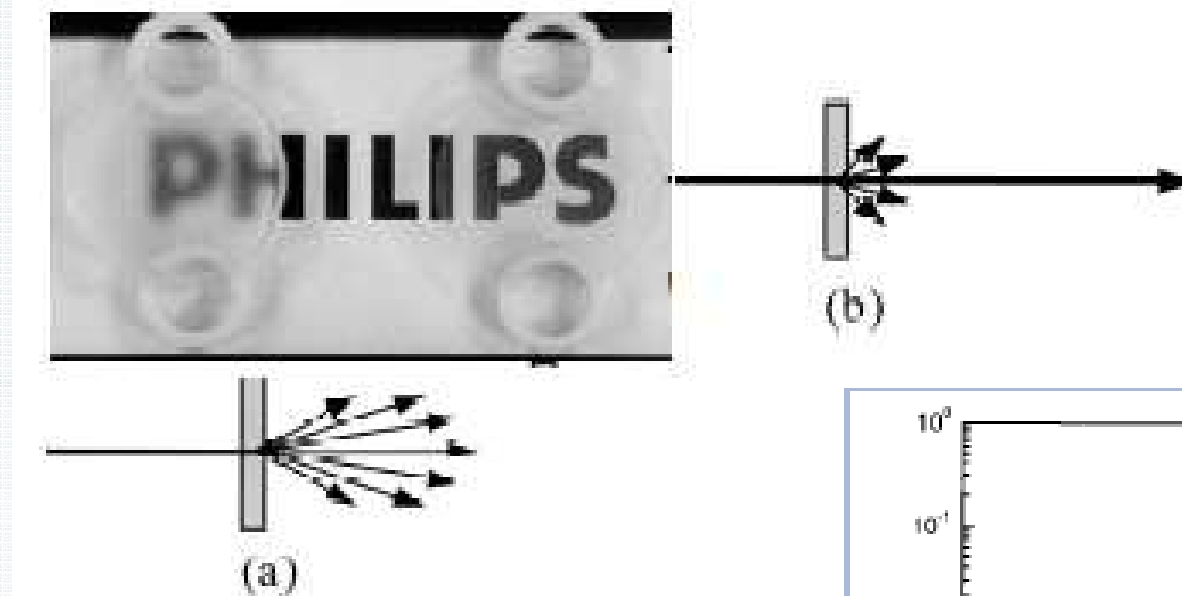


Plate bonding – Composite materials



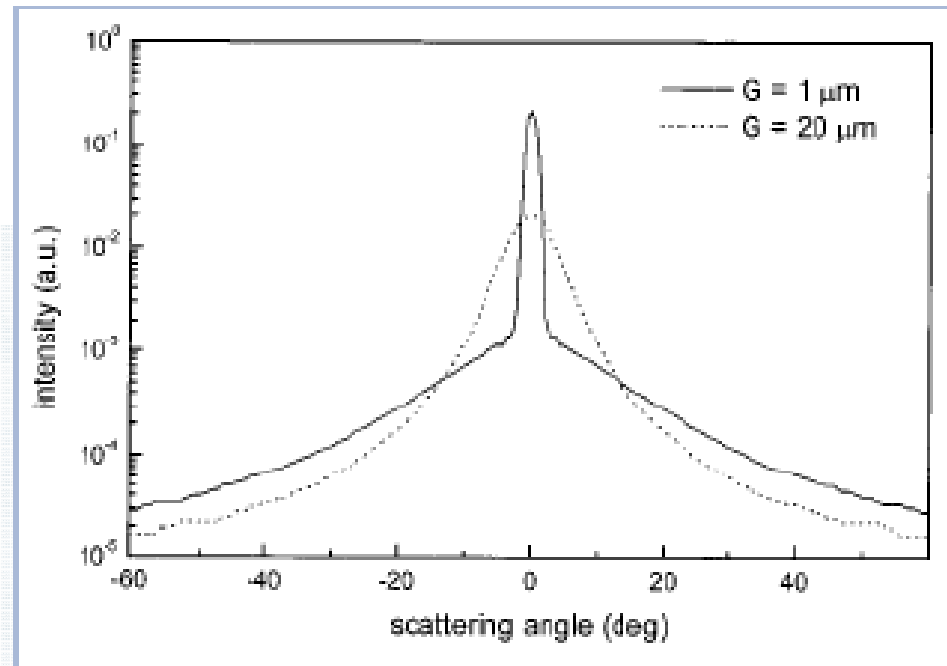
Photo of the composite, all ceramics passively Q-switched Nd: YAG/Cr:YAG with three beam output

Dependence of transparency of grain size

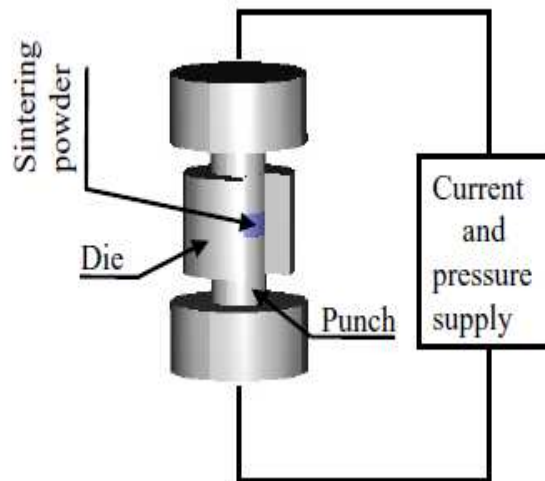


Optical transparency are highly influenced by grain size.

Large grain sizes create diffuse/ multi scattering.



SPARK PLASMA SINTERING (SPS)



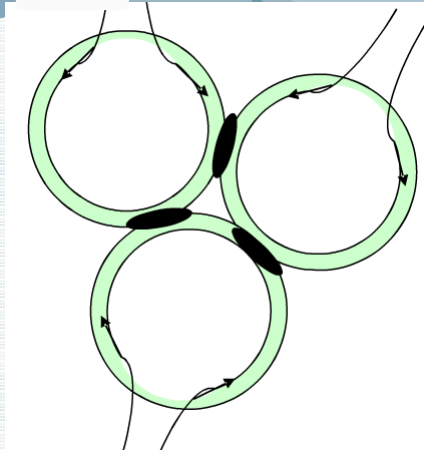
- ❑ Method developed to obtain fully dense and fine-grained transparent ceramics at low temperatures within short duration of time
- ❑ Also known as field assisted sintering or pulsed electric current sintering.
- ❑ SPS uses a high density current flux through the sample and the die to cause Joule heating within the sample.
- ❑ High heating rate is another important highlight of SPS.

Disadvantages: Carbon contamination from the die set-up

Few examples of transparent ceramics fabricated by SPS:

Rare earth doped Sesquioxides, Garnet, YAG, Al_2O_3 , ZnO, ZrO_2 , PMN-PT

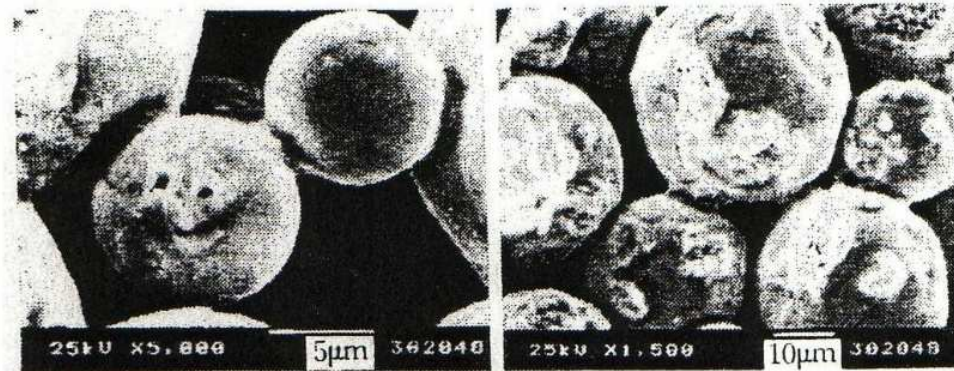
Detailed mechanisms involved in SPS is presented in the preceding slides



Joule's heating: localized temperature increment



Sintering activated

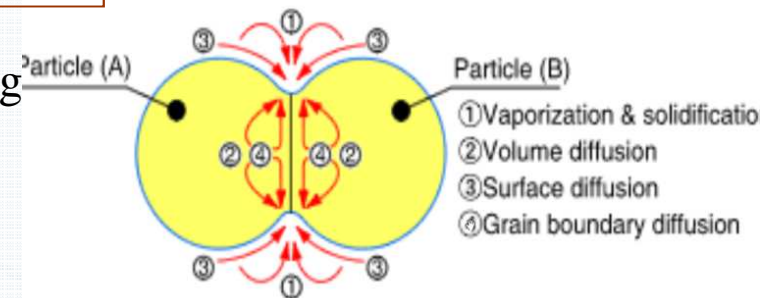


Neck formation due to localized heating

Groza et al., UC Davis

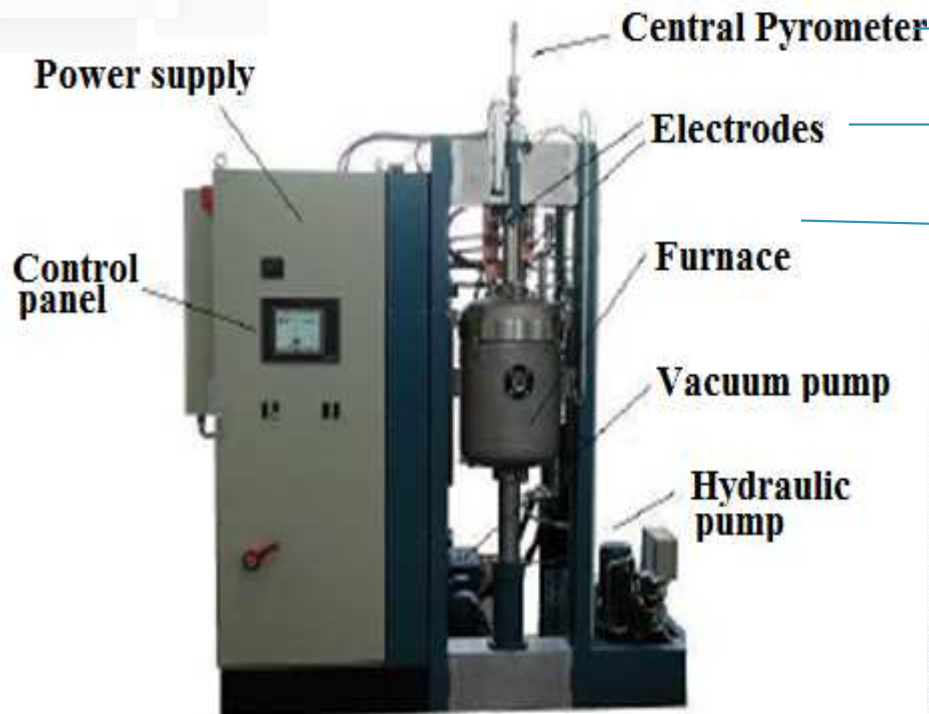
Three mechanisms that contribute to spark plasma sintering

- (a) Activation of powder particles by pulsed current
- (b) Resistance sintering
- (c) Pressure application



❑ In the presence of Pressure and electric current, localized necking occurs faster due to Joule heating.

❑ Consequently temperature raises very fast (faster than conventional sintering and hot pressing) and the densification is completed within few minutes.



hot pressing

Main differences:

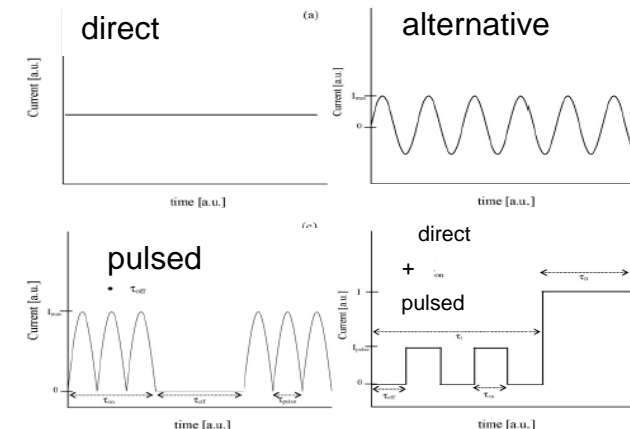
1. Heating modes and heating rates

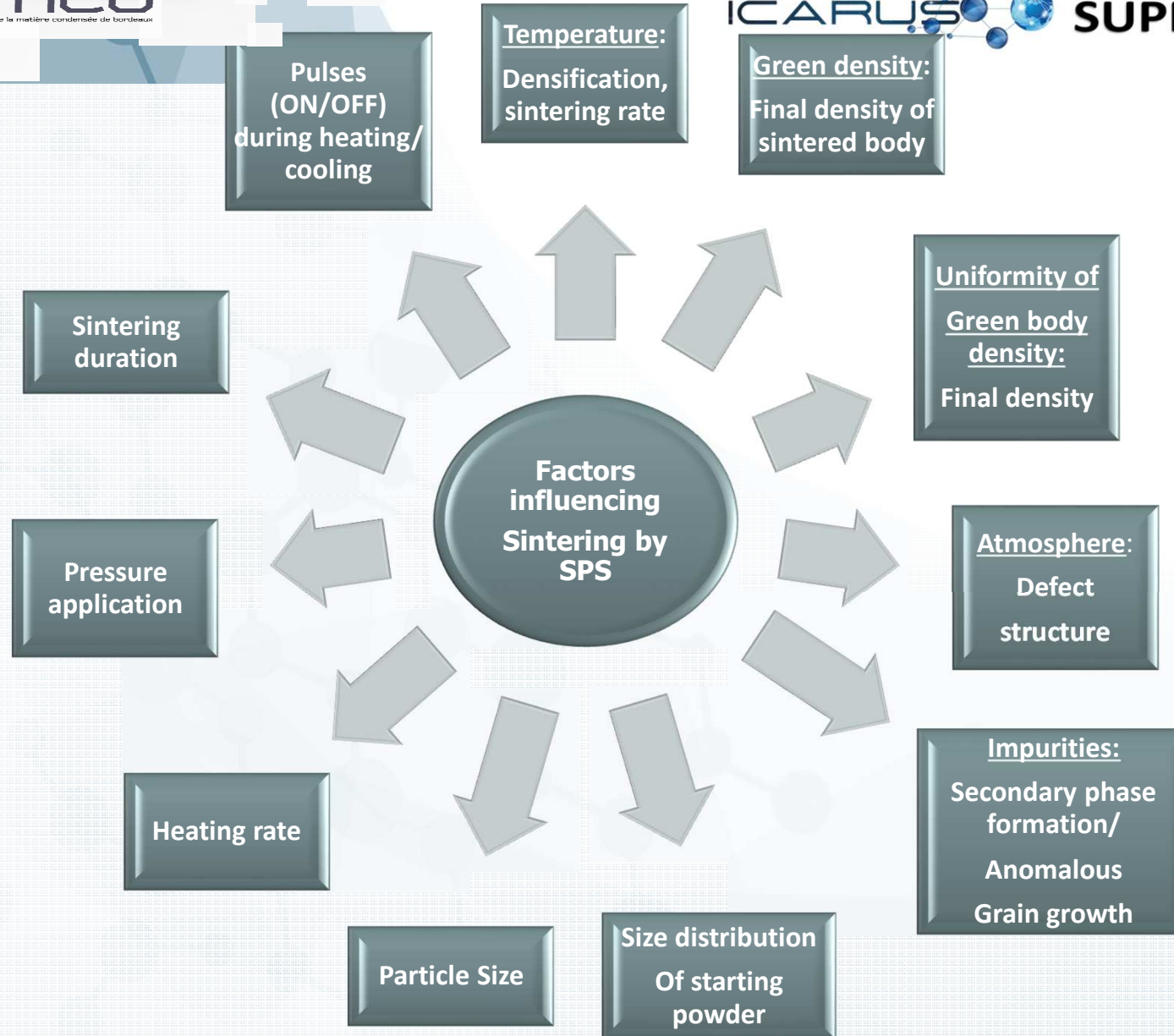
- ❑ SPS: Joule effect \rightarrow 1000°C/min (250°C/min)
- ❑ Hot pressing: a) Inductive heating: 150°C/min (100°C/min)
b) Resistive heating: 50°C/min (10°C/min)

2. Pulses (3.3ms) or continuous current

Spark plasma sintering

K. Umi et al./ Materials Science and Engineering K 63 (2009) 147–207





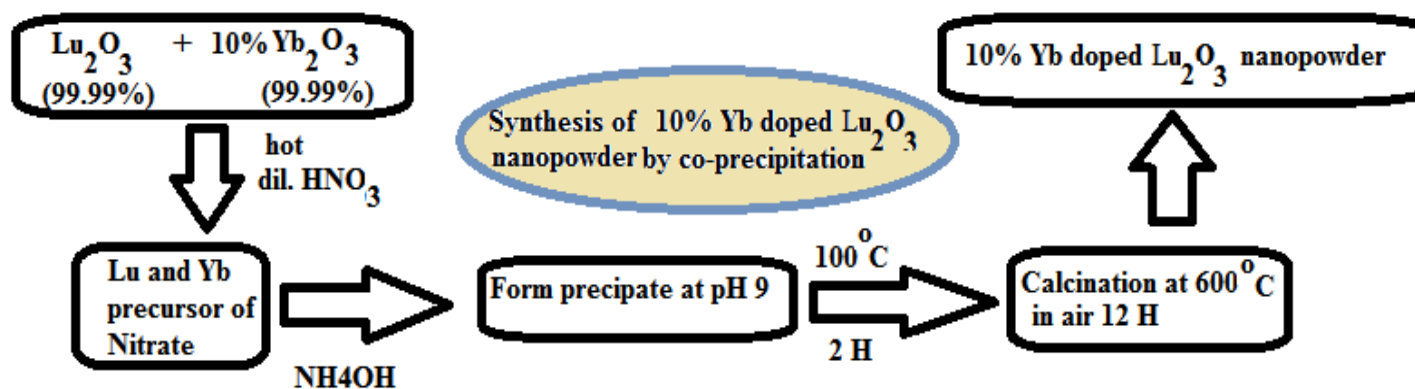
FEW EXAMPLES FROM RESEARCH WORK ON TRANSPARENT CERAMICS BY SPS AT ICMCB

- 1. Cubic / isotropic Crystalline structured materials: Sesquioxides**
- 2. Non cubic / anisotropic Crystalline structured materials: Alumina**

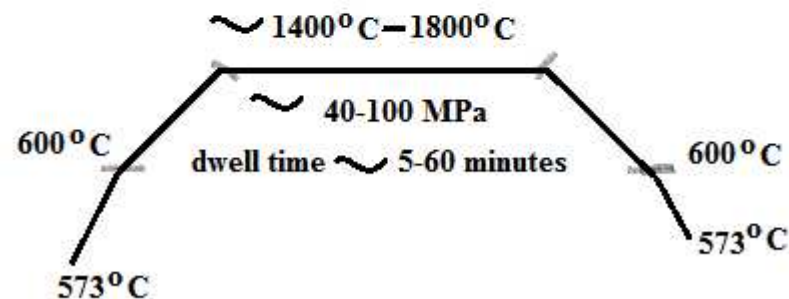
How the sintered parameters could help us to control the microstructure and then the final properties

Cubic / isotropic Crystalline structured materials

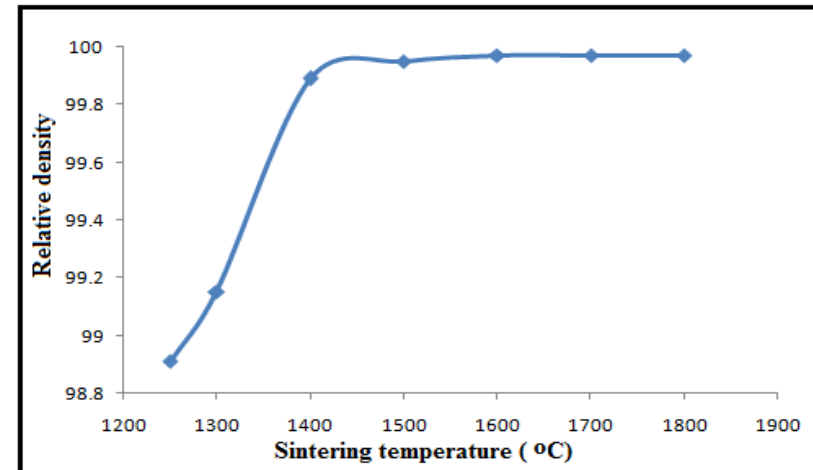
10% Yb doped Lu_2O_3 – Cubic system- our experimental studies



Dr. Sinter lab Spark Plasma Sintering system,
model SPS-511S/SPS-515S
Vacuum= 10^{-3} torr
Pulse sequence for SPS
applied voltage = 12: 2
Heating rate & cooling rate = $5^\circ\text{C}/\text{minute}$ - $200^\circ\text{C}/\text{minute}$
Pressure= 40 -100 MPa
Dwell time= 5- 60 minutes



Dependence of relative density on sintering temperature at $P_s = 100 \text{ MPa}$, $t_s = 5 \text{ min}$



❑ Effect of Pressure

➤ Sintering curves of YLO bodies strongly dependent on the preload pressure (P_0) :

1) by applying constant maximum pressure (P_s) in the entire process. 2) by applying P_s only during the dwell time (t_s): best result

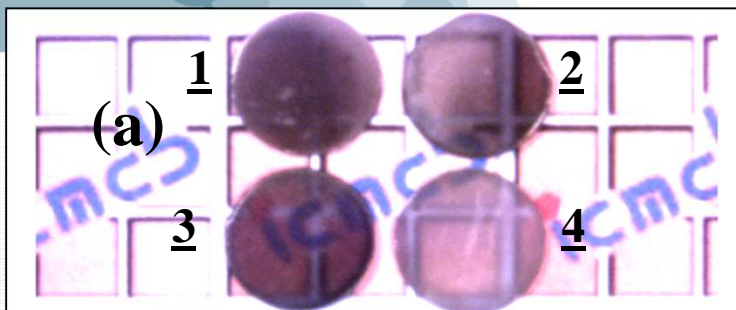
❑ Effect of sintering temperature

➤ **Maximum densification was reached at 1350°C**, above this temperature, the densification increases very little

❑ Effect of heating rate

➤ **Average size of the grain increases rapidly with increasing heating rate (R_H)**, leading to **inhomogeneous grain size distribution** inhibiting transparency of the ceramic : optimal R_H to yield transparent YLO ceramics determined to be $R_H = 50^\circ\text{C}/\text{min}$.

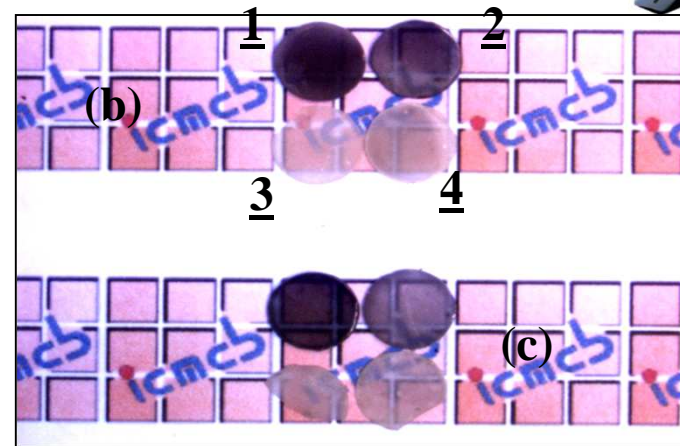
(M. Prakasam et al. / Ceramics International 39 (2013) 1307–1313)



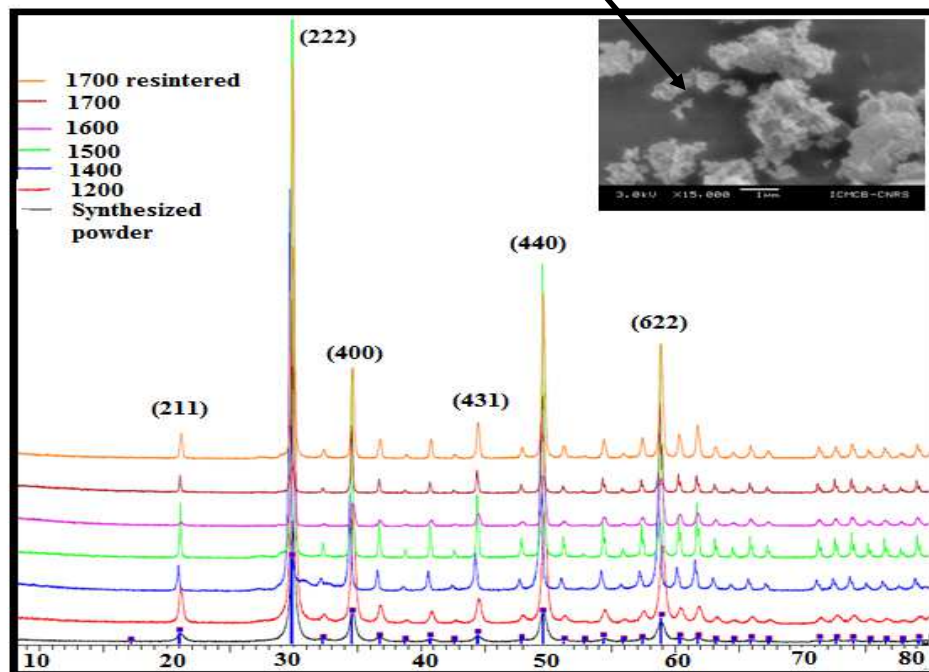
10%Yb₂O₃ doped Lu₂O₃ ceramics sintered at 1700°C Ps=100MPa

- (a) 1. R_H= 10°C/min t_s= 20 min
 2. R_H= 10°C/min t_s= 5 min
 3. R_H= 50°C/min t_s= 20 min
 4. R_H= 50°C/min t_s= 5 min

Starting powder: $\phi \approx 10$ nm

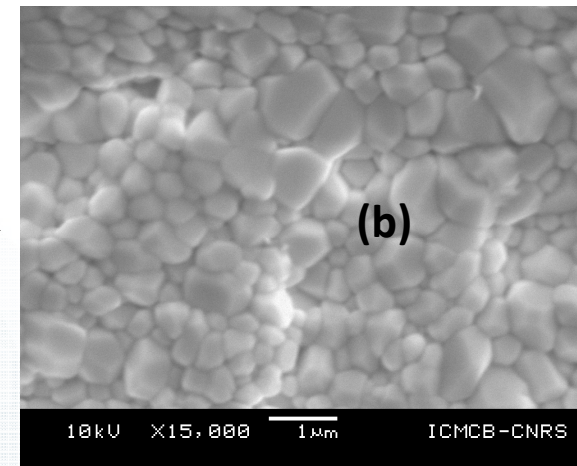
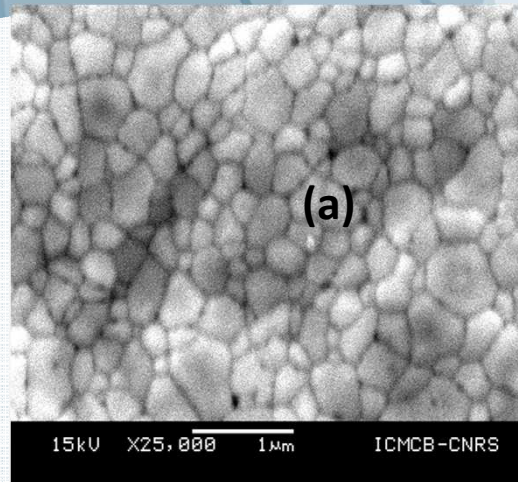


(b) and (c) are the corresponding samples compared with annealed samples at 1200°C for 12 h (oxygen vacancies, C)



- Unit cell parameter for YLO : $a = 10.402 \text{ \AA}$ \Rightarrow slight increase than the value of Lu₂O₃ cell parameter, due to the incorporation of the Yb in the crystal structure of Lu₂O₃
- In the whole temperature range (1400°C-1800°C) of analyses chosen for investigation \Rightarrow no additional phases or decomposition have been observed.

(M. Prakasam et al. / Ceramics International 39 (2013) 1307–1313)



SEM micrographs of ceramics :

(a) 1700°C, 100MPa, $t_s = 5\text{min}$ and $R_H = 50^\circ\text{C/min}$

(b) 1700°C, 100MPa, $t_s = 5\text{min}$ and $R_H = 50^\circ\text{C/min}$, annealed at 1200°C for 12 h

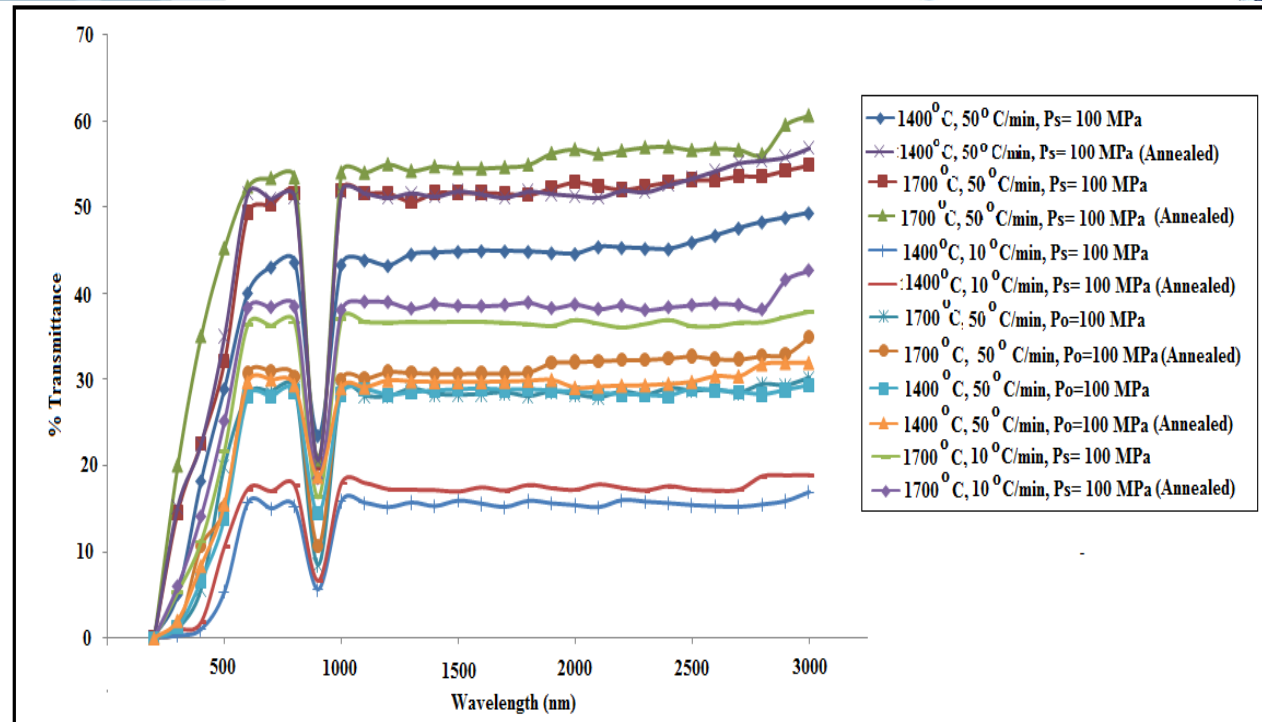
❑ Over the temperature range of 1400°C-1800°C, with $P_s = 100\text{MPa}$, $R_H = 50^\circ\text{C/min}$ and $t_s < 20\text{min}$, the grain grew uniformly, with distinct grain boundaries.

❑ Porosity (Archimedes) of YLO ceramics decreases with increasing temperatures and increasing holding time, while the applied pressure has little effect on the porosity.

(M. Prakasam et al. / *Ceramics International* 39 (2013) 1307–1313)



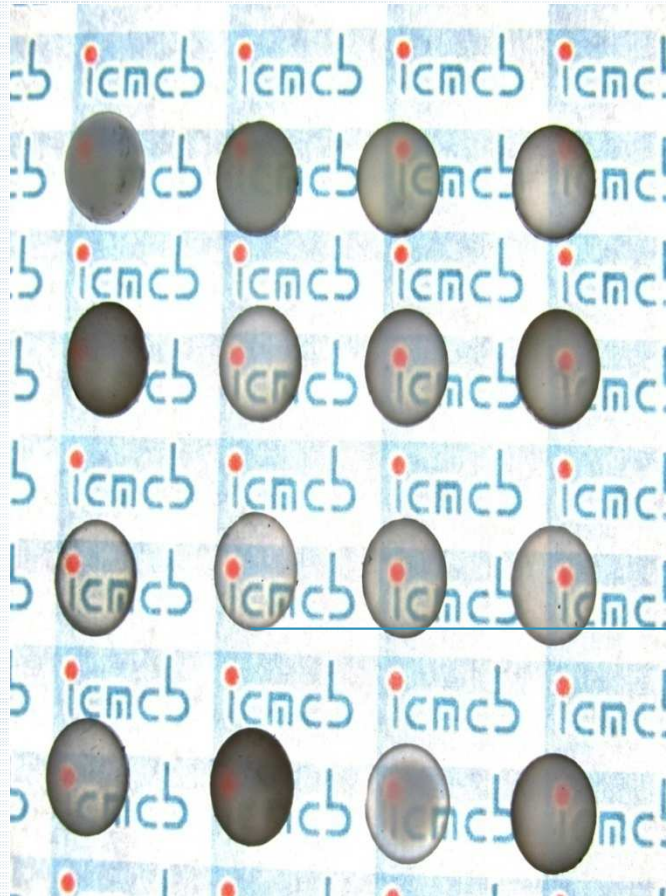
**Transmittance spectrum
of sintered transparent
ceramics under different
sintering conditions by
spark plasma sintering**



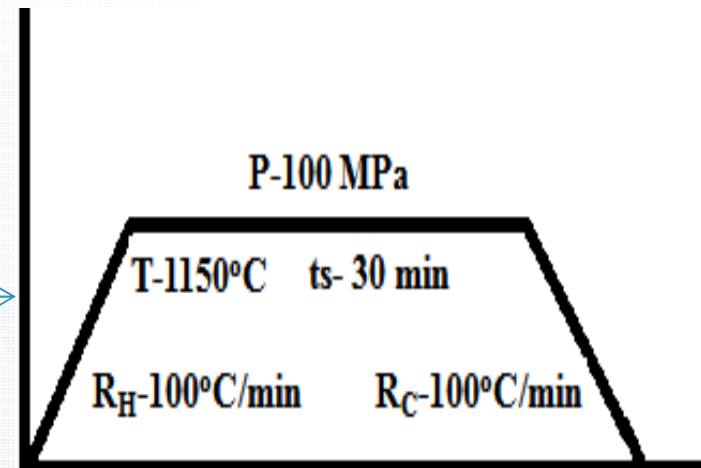
→ The samples sintered at **1700°C for 5 minutes** exhibited higher transparency than that of the ceramics sintered at 1400°C.

→ The increasing transmission with sintering temperature may be attributed due to densification.

→ The YLO ceramics fabricated at 1700°C and 1400°C **had nearly 5-10% improvement in transmittance upon annealing at 1200°C for 12 h.**



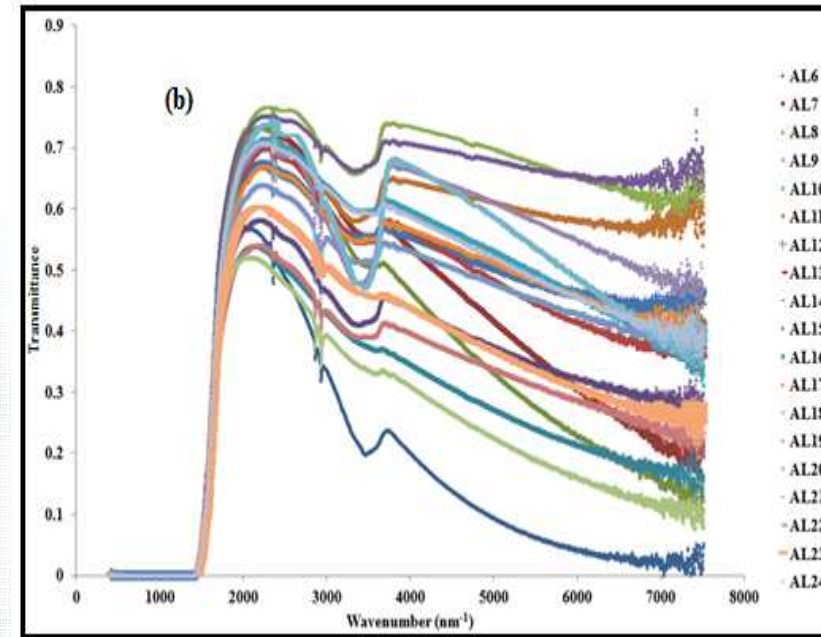
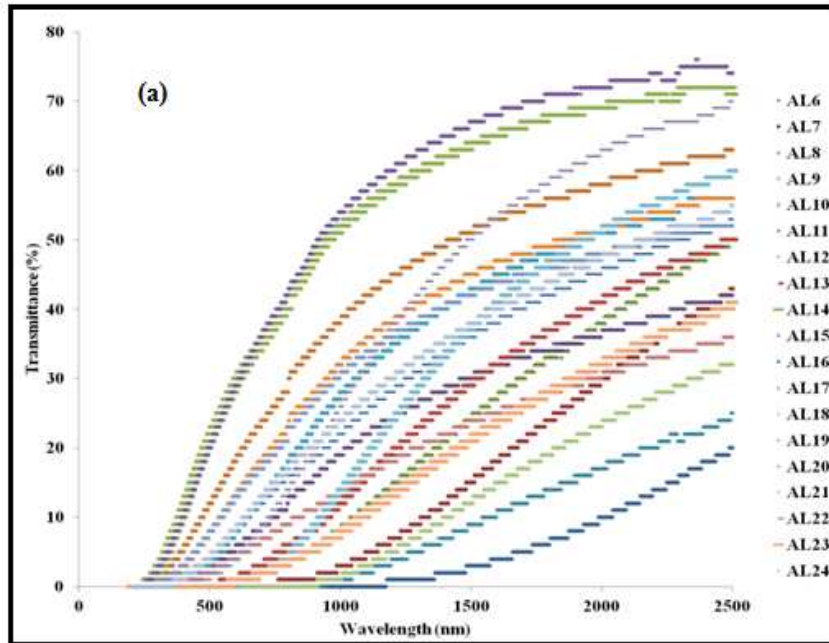
Transparent Al_2O_3
ceramics for Armor and
IR applications



M. Prakasam et al. / Journal of European Ceramics society (Accepted) 2014

Noncubic / anisotropic Crystalline structured materials

Optical Characterization of PCA obtained by SPS



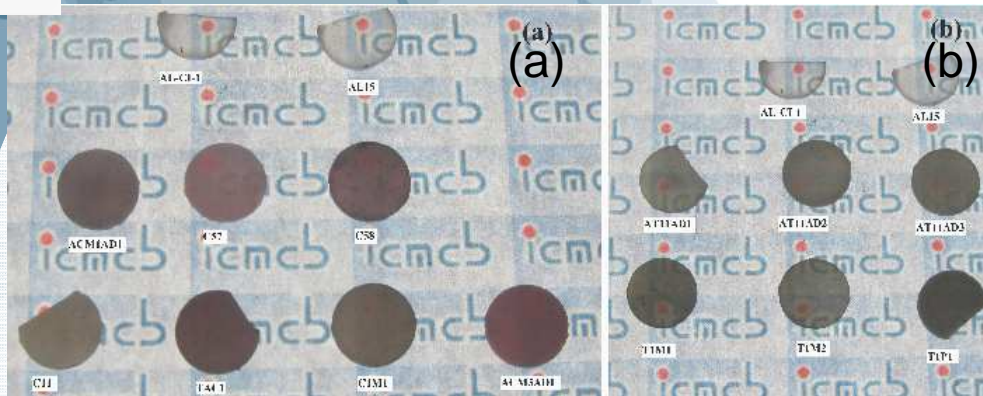
Transmittance spectra of PCA ceramics in (a) UV-Visible region and (b) Infra-red region (thickness 2mm)

→ Maximum transmission of alumina has been achieved by other techniques such as pressureless sintering, followed by HIP, Its transmission is very close to that of saphir single crystal and remains **at 86% in the wavelength range of 3-4.5 μm for a thickness of 1mm.**

→ It can be inferred that the transmittance of PCA increases in UV-Visible-NIR and mid-IR with the increasing dwell time, pressure and heating rate.

→ Further the application of pressure (100 MPa) at the start of sintering cycle decreases the transmittance of the PCA ceramics to 10% lesser than the application of pressure at the dwell time.

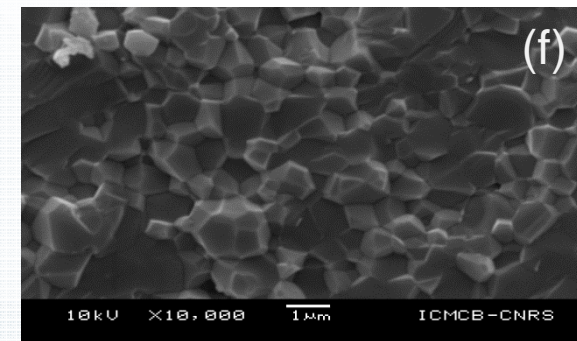
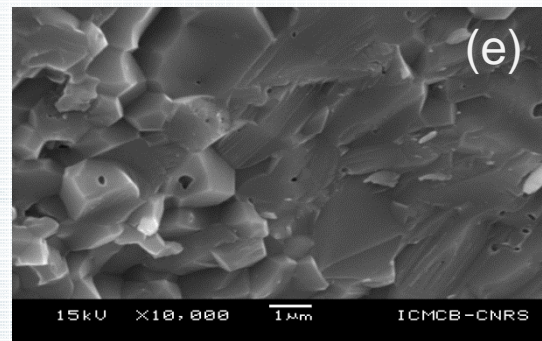
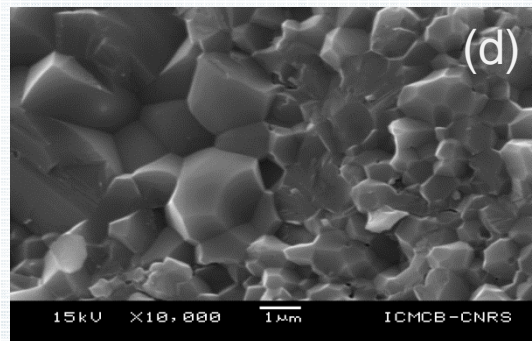
Control of grain growth (Al_2O_3 doped with Cr_2O_3 and Ti_2O_3) by additive to avoid abnormal grain growth upon sintering



(a) Al_2O_3 doped with Cr_2O_3 sintered at different sintering conditions
(b) Al_2O_3 doped with Ti_2O_3 sintered at different sintering conditions



(c) Al_2O_3 doped with Cr_2O_3 and Ti_2O_3 sintered by addition of 0.05 Wt% of MgO



Microstructures of Al_2O_3 doped with Cr_2O_3 at 1300°C with dwell time of 20 minutes (d) heating rate 10°C/min (e) heating rate 100°C/min and (f) heating rate 10°C/min with addition of 0.05 Wt% MgO

- **Effectiveness of the additive to suppress grain growth** is often found to depend on its ability to segregate at the grain boundaries.
- **Inhibition of grain growth** is believed to occur by a mechanism of solute drag. A Strong interaction occurs between the segregated solute and the grain boundary so that the solute must be carried along with the moving boundary.
- Solute diffusion across the boundary is assumed to be slower than that of host atoms and therefore becomes rate controlling.

Transparent ceramics fabricated at ICMCB by SPS



Translucent ZnO
ceramics on Silicon
substrate by SPS for
LED applications
Product developed for
company Nanovation,
Paris at ICMCB



HAp Sintering
temperature = 850°C,
Dwell time= 10 min



Zirconia Sintering
temperature =
1200°C,
Dwell time= 20 min

$\text{AgGaGe}_5\text{Se}_{12}$

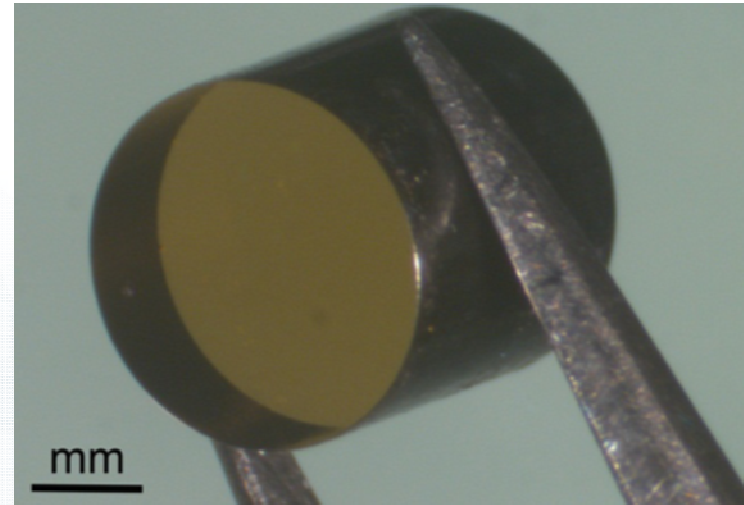


$\text{AgGaGe}_3\text{Se}_8$

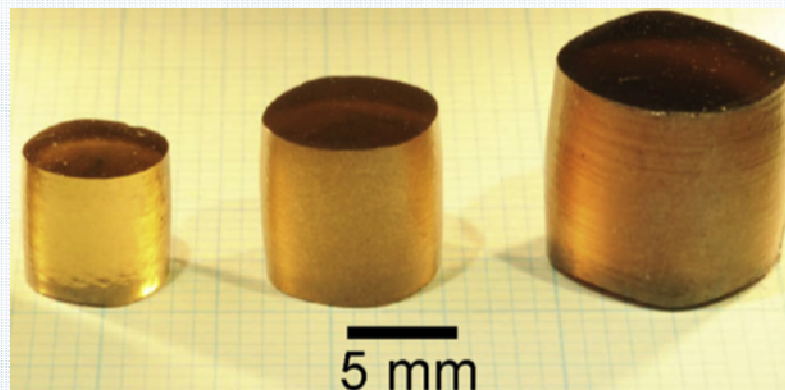


Silver based Chalcogenides for
mid-IR applications

Few examples of transparent PCD to date in literature



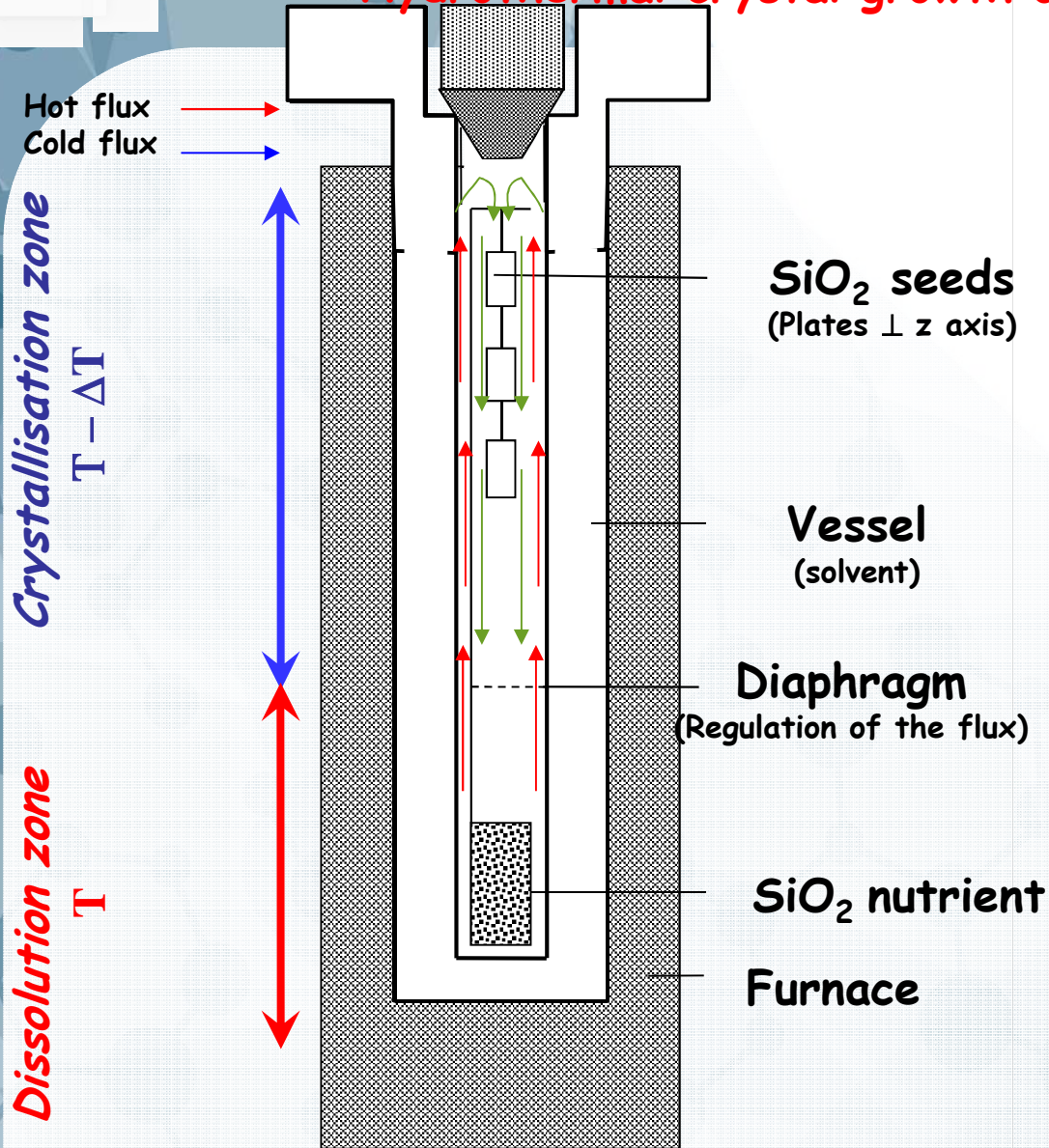
K. Harano et al. / *Diamond & Related Materials* 24 (2012) 78–82 Y.-Y. Chang et al. / *Physics of the Earth and Planetary Interiors* 228 (2014) 47–55



T. Irifune et al. / *Physics of the Earth and Planetary Interiors* 228 (2014) 255–261

Hydrothermal crystal growth of SiO_2

Principle



Dissolution of nutrient by the solvent
in the hot zone (bottom)

($T_{\text{dissolution}}$)



Creation of solvated species



Saturation of the solution
In the dissolution zone



Transport (convection) of the solvated species
from the hot zone (bottom) to the cold zone
(top)



Supersaturation of the solution
in the crystallization zone

($T_{\text{crystallization}} < T_{\text{dissolution}}$)



Deposition on the seed

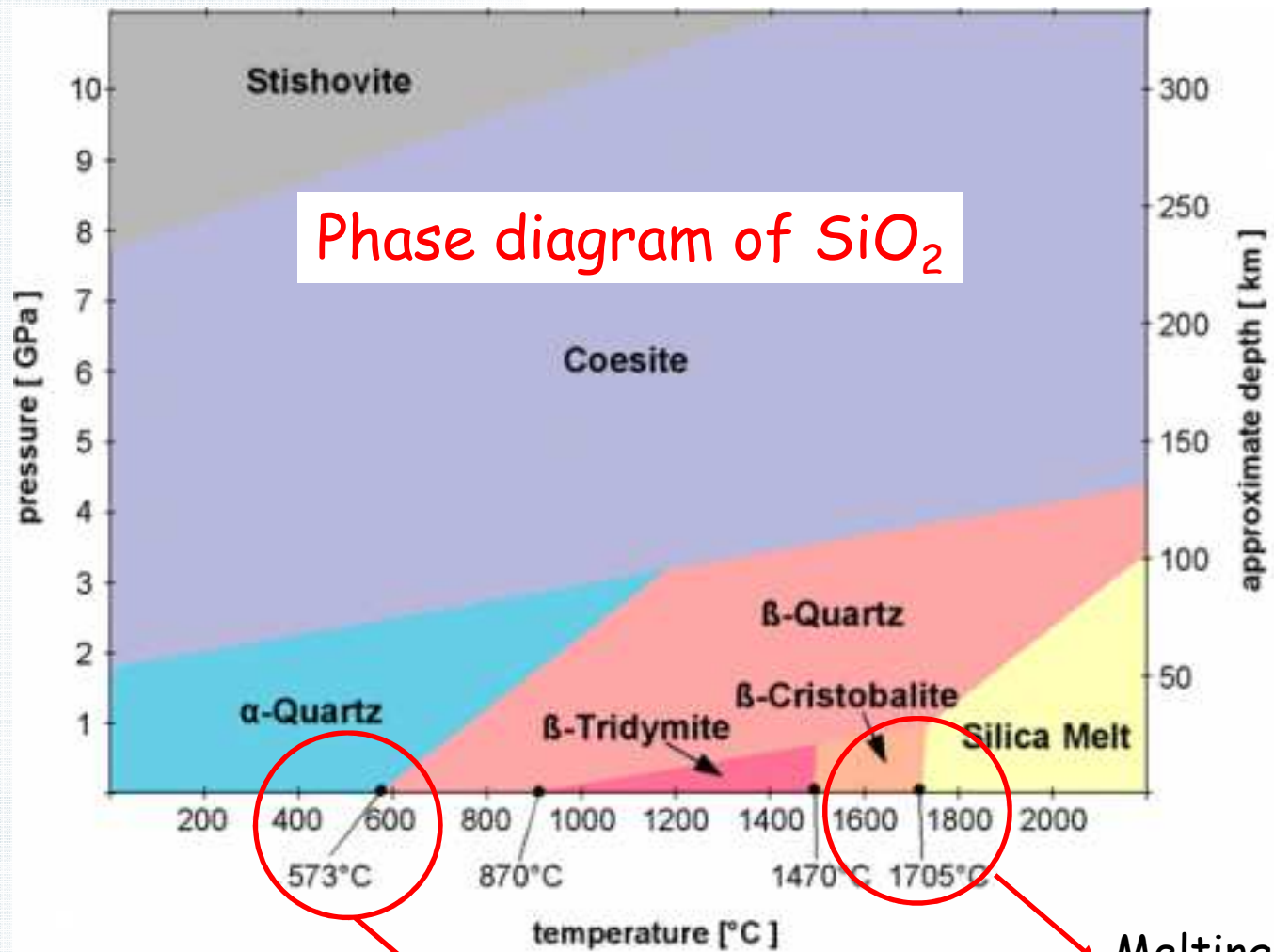


Impoverishment of the solution which descend
to the bottom (re-saturated solution)
and the cycle re-start

Effect of P = Increase and manage the solubility of precursor « nutrient »

Effect of ΔT = Create a difference of solubility generating a transport of species from hot to cool zone

Hydrothermal Crystal Growth and Structural Studies of $\text{Si}_{1-x}\text{Ge}_x\text{O}_2$ Single Crystals



α - Quartz / β - Quartz

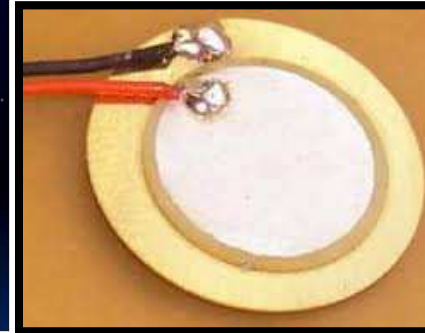
Melting



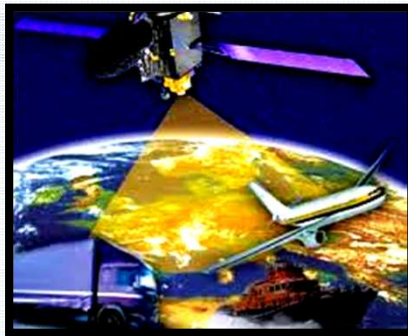
Pacemakers



Celestial navigation

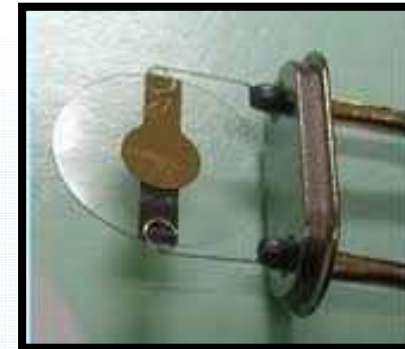


Piezoelectric transducers

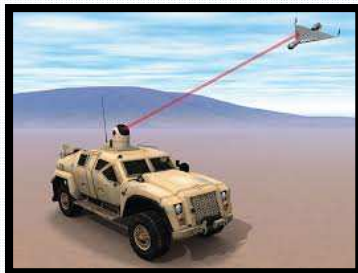


GPS system

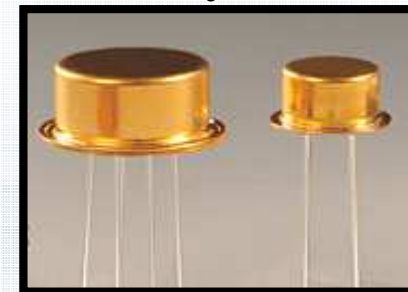
**Few examples of
Quartz Crystal
applications**



Quartz crystal microbalance



Military and aerospace navigation

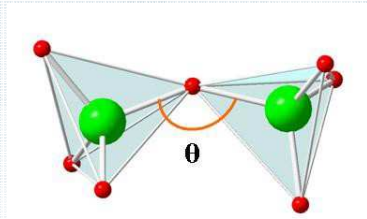


Precise frequency controller

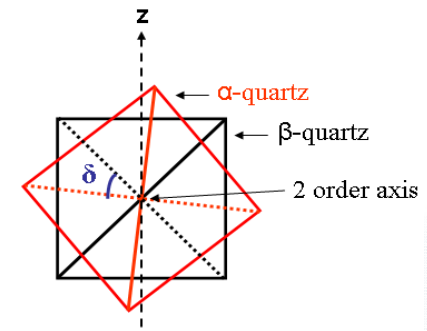
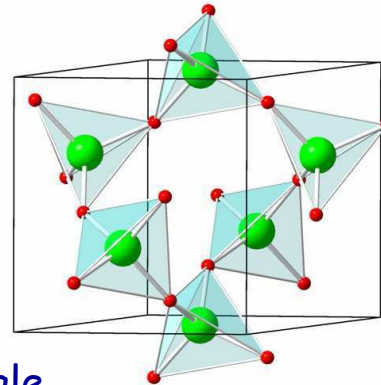
Trigonal system
Space group: $P3_121$ (right) or $P3_221$ (left)

Lattice parameters : $a = 4,913\text{\AA}$ $c = 5,405\text{\AA}$

Helical chain of tetrahedral along the z axis



θ : inter-tetrahedral bridging angle



δ : tetrahedral tilt angle

α -quartz: $\theta = 143.6^\circ$ and $\delta = 16.2^\circ$

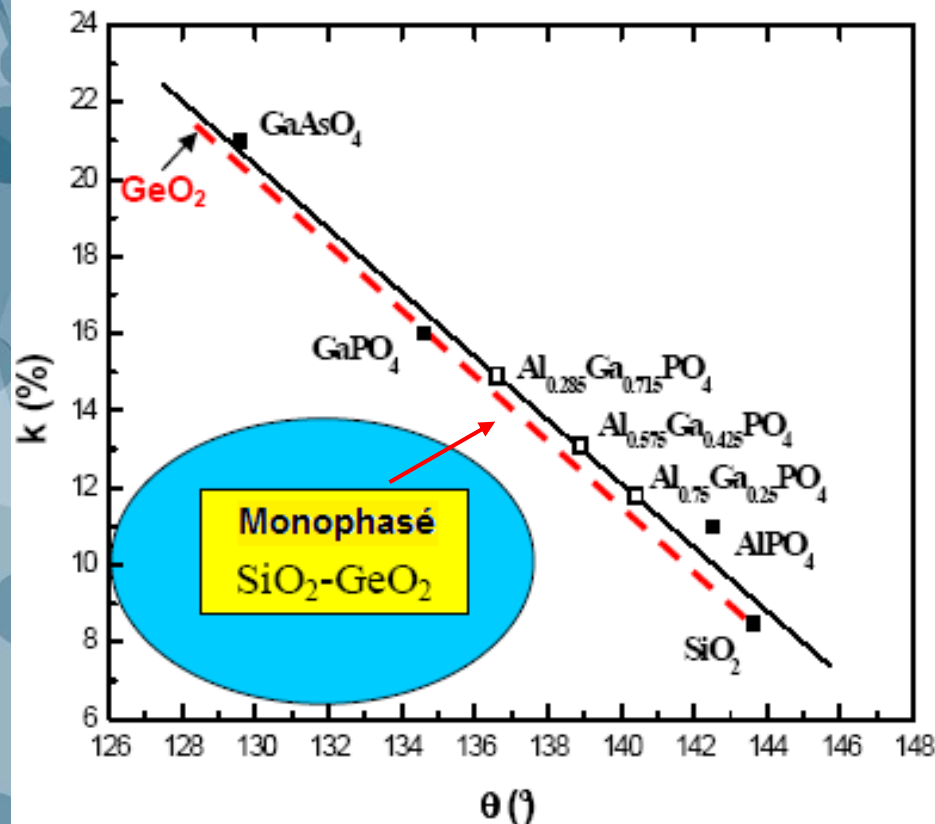
\Rightarrow Electromechanical coupling coefficient $k \approx 8\%$

β -quartz: $\theta = 154^\circ$ and $\delta = 0^\circ$

\Rightarrow Electromechanical coupling coefficient $k \approx 0\%$

If $\theta \downarrow$ or $\delta \uparrow \Rightarrow$ distortion (/ β -quartz) \uparrow

Relation between θ (distortion) and k



AlPO₄: α -quartz homotype



Substitution Al / Ga



(size: $\text{Ga}^{3+} \gg \text{Al}^{3+}$)



$\theta \uparrow$ (distortion \uparrow) if at.% Ga \uparrow



$k \uparrow$

E. Philippot et al., *J. solid state chemistry* 1996, 123, 1



SiO₂ : Substitution Si / Ge (size: $\text{Ge}^{4+} \gg \text{Si}^{4+}$) $\Rightarrow \text{Si}_{1-x}\text{Ge}_x\text{O}_2$

Existence of SiO_2 - GeO_2 domain

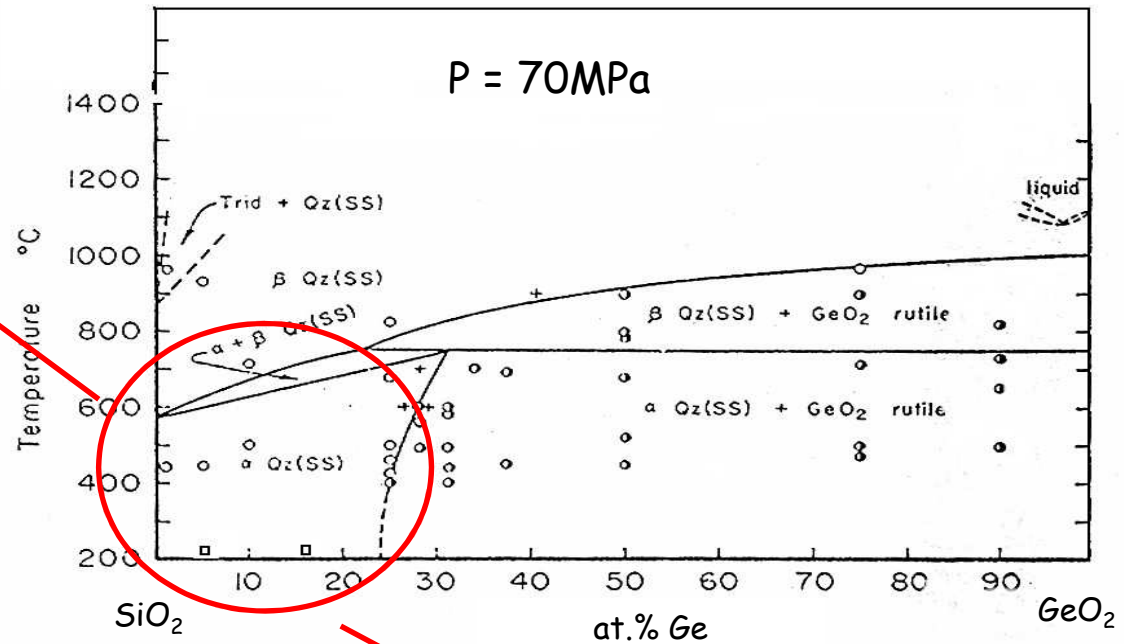
31at.% Ge at 700°C and 70 MPa
in SiO_2 α -quartz



Phase rutile like = tetragonal
 $P4_2/mnm$

↓ 1033°C ↓

α -quartz like = trigonal
 $P3_221$



No information at ambient temperature



Single crystal of $\text{Si}_{1-x}\text{Ge}_x\text{O}_2$

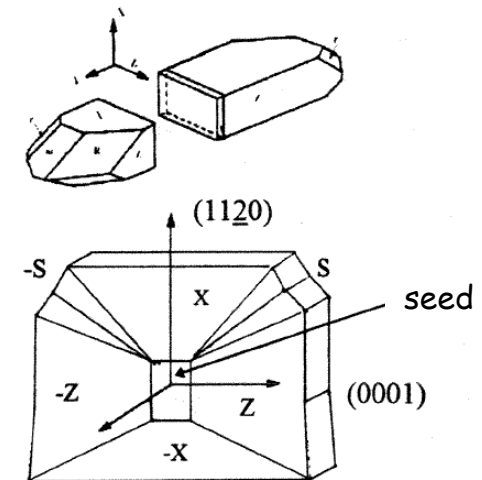
With x (at. %) max ?



SiO_2 α -quartz Hydrothermal Crystal Growth

SiO_2 α -quartz hydrothermal crystal growth

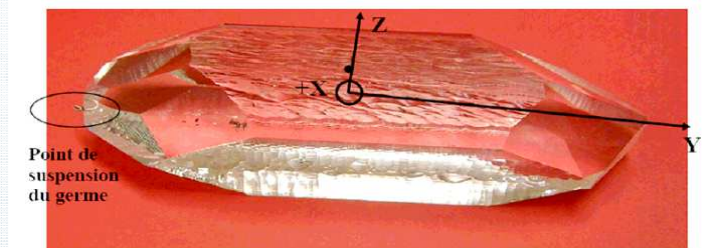
Parameters	High Pressure	Low Pressure
Temperature	360°C	345°C
Pressure	150 MPa	70-100 MPa
Gradient	25°C	10°C
Solvent	NaOH 1M	Na ₂ CO ₃ 0.8M
Growth rate (sur Z)	1mm/day	0.4mm/day



$\text{Si}_{1-x}\text{Ge}_x\text{O}_2$ α -quartz hydrothermal crystal growth

- Seed: SiO_2 α -quartz (no other choice)
- Solvent: NaOH, Na₂CO₃, H₂O, .. (depending of the solubility)
- Nutrient: SiO_2 + GeO_2 (depending of the solubility)
- Pressure: lowest possible
- Temperature : lowest possible

} **Industrial application**

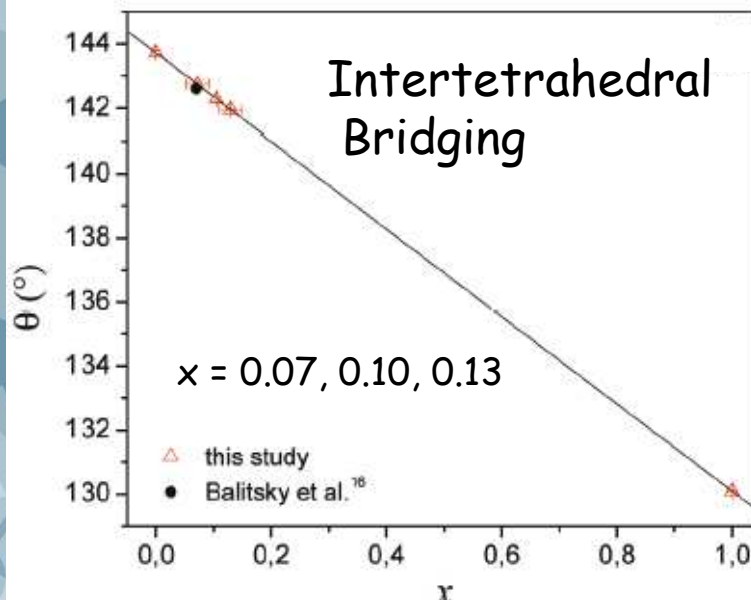


Structural distortion on crystals

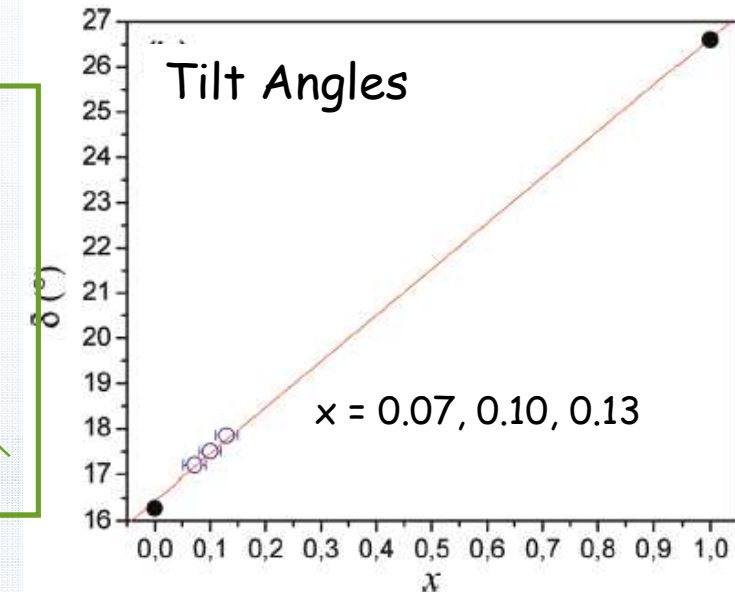
	SiO ₂	Si _{0.93} Ge _{0.07} O ₂	Si _{0.87} Ge _{0.13} O ₂	GeO ₂
a (Å)	4.9137 (8)	4.9200 (2)	4,9222 (2)	4.9853 (1)
c (Å)	5.4047(12)	5.4195 (2)	5,424 (1)	5.6450 (1)
c/a	1.0999	1.1014	1,102	1.1323
V (Å ³)	113.01 (5)	113.61 (1)	113,82 (1)	121.50 (1)
Angle θ (°)	143.6 (1)	142.75 (5)	141,95 (1)	130.05 (4)
Angle δ (°)	16.28 (6)	17.21 (2)	17,85 (3)	26.61 (4)

If $x \uparrow$

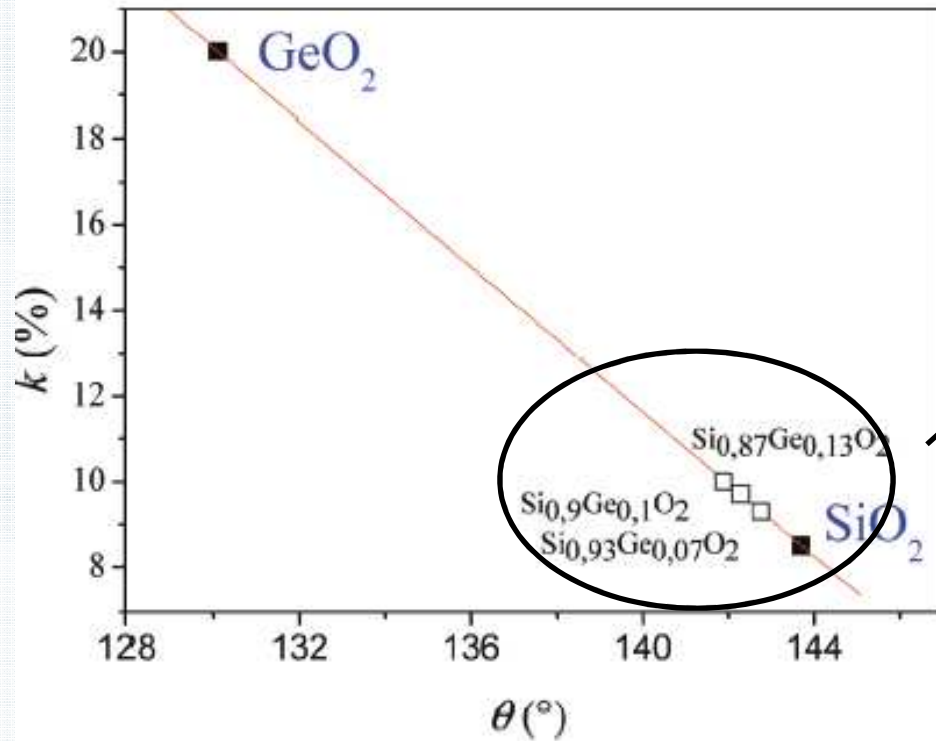
Inter-tetrahedral Bridging and Tilt Angles in Si_{1-x}Ge_xO₂ α -quartz



If $x \uparrow$
 \Downarrow
 $\theta \downarrow$ and $\delta \uparrow$
 \Downarrow
 distortion \uparrow



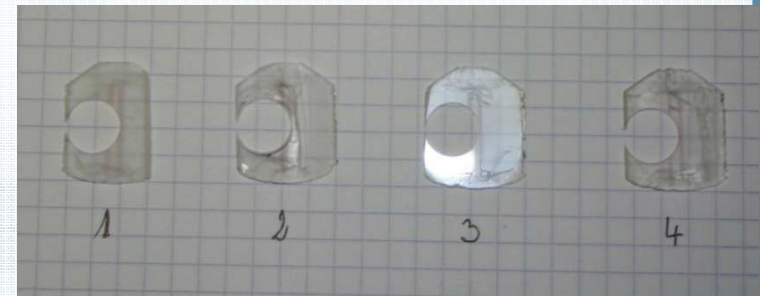
Expected Piezoelectric coupling coefficient k



predicted k values for $\text{Si}_{1-x}\text{Ge}_x\text{O}_2$ crystals with $x = 0.07, 0.10, 0.13$ function of inter-tetrahedral bridging angle



Next step
discs for
resonators



Applications of hydro(solvo)thermal crystal growth

• In industrial scale:

- **SiO₂ (α -quartz)** (**NaOH, Na₂CO₃**): piezoelectric properties (oscillators, resonators, transducers) and optics (filters)
- **ZnO** (**KOH, NaOH**): semi-conductor transparent, dielectric and piezoelectric)
- **CaCO₃** (**NaCl, Ca(NO₃)₂, K₂CO₃**, 150-600°C / 15-200MPa): Optical properties (birefringence and transmission in the large spectral domain)
- **KTiOPO₄ (KTP)**: (**K₂HPO₄+KH₂PO₄+H₂O₂/KTP (425-600°C / 70MPa)**): non linear optical properties (lasers)
- **GaN (NH₃)** : Evaluation of solvothermal crystal growth using mineralizers base (NaNH₂ or LiNH₂) or acidic (NH₄Cl) (2007-2008) \Rightarrow Japan
- **Diamond** (**Molten metallic medium**) \Rightarrow Japan
- Precious stones: amethyst (purple colored quartz Fe³⁺ + irradiation), citrine (colored quartz Fe²⁺), blue quartz (doping Co²⁺), smoky quartz black "morion" (Al³⁺ + irradiation), ruby (red Al₂O₃:Cr) , sapphire (Al₂O₃ other colors: Ni, Cr, Co, ..), emerald (Beryl: Be₃Al₂Si₆O₁₈:Cr)

• In Research scale:

- piezoelectric materials comparable to α -Quartz
 - Berlinite: α -AlPO₄ ($T_{\alpha \rightarrow \beta}$: 584°C) and GaPO₄ ($T_{\alpha \rightarrow \beta}$: 976°C: H₃PO₄, H₂SO₄, HCl, HNO₃)
 - GaAsO₄,
 - Langasite
- **GaN**: Nutrient **Li₃GaN₂** forming **GaN₂³⁻** in NH₃ (*Thèse A. DENIS Univ. Bx 2003*)

Thank you!



The ICARUS project has received funding from the European Union's Horizon 2020 research and innovation programme under grant agreement No 713514.

The SUPERMAT project has received funding from the European Union's Horizon 2020 research and innovation programme under grant agreement No 692216.

This document and all information contained herein is the sole property of the ICARUS and SUPERMAT Consortiums or the company referred to in the slides. It may contain information subject to Intellectual Property Rights. No Intellectual Property Rights are granted by the delivery of this document or the disclosure of its content.

Reproduction or circulation of this document to any third party is prohibited without the written consent of the author(s).

The statements made herein do not necessarily have the consent or agreement of the ICARUS and SUPERMAT consortiums and represent the opinion and findings of the author(s).

The dissemination and confidentiality rules as defined in the Consortium agreement apply to this document.

All rights reserved ®

